Indirect Formation of Peptide Bonds as a Prelude to Ribosomal Transpeptidation

Harvey J. A. Dale* and John D. Sutherland*

MRC Laboratory of Molecular Biology, Francis Crick Avenue, Cambridge, CB2 0QH, United Kingdom

Prebiotic chemistry, peptide synthesis, reaction mechanism, ribosomes, translation, aminoacyl esters, transfer RNA

ABSTRACT: The catalytic competency of the ribosome in extant protein biosynthesis is thought to arise primarily from two sources: an ability to precisely juxtapose the termini of two key substrates – 3'-aminoacyl and *N*-acyl-aminoacyl tRNAs – and an ability to ease *direct* transpeptidation by their desolvation and encapsulation. In the absence of ribosomal – or enzymatic – protection, however, these activated alkyl esters undergo efficient hydrolysis, whilst significant entropic barriers serve to hamper their *inter*molecular cross-aminolysis in bulk water. Given that the spontaneous emergence of a catalyst of comparable size and sophistication to the ribosome in a prebiotic RNA world would appear implausible, it is thus natural to ask how appreciable peptide formation could have occurred with such substrates, in bulk water, *without* the aid of advanced ribozymatic catalysis. Using a combination of fluorine-tagged aminoacyl adenylate esters, *in situ* monitoring by $^{19}F\{^{1}H\}$ NMR spectroscopy, analytical deconvolution of kinetics, pH-rate profile analysis, and temperature-dependence studies, we here explore the mechanistic landscape of *indirect* amidation, *via* transesterification and *O*-to-*N* rearrangement, as a highly efficient, alternative manifold for transpeptidation that may have served as a prelude to ribosomal peptide synthesis. Our results suggest a potentially overlooked role for those amino acids implicated by the cyanosulfidic reaction network with hydroxyl side chains (Ser, Thr), and they also help to resolve some outstanding ambiguities in the broader literature regarding studies of similar systems (e.g. aminolyses with Tris buffer). The evolutionary implications of this mode of peptide synthesis, and the involvement of a very specific subset of amino acids, are discussed.

INTRODUCTION

The coded biosynthesis of proteins – the translation of genetic information into function – is a defining pillar of molecular biology, and an apparent prerequisite for something as sophisticated as life. At the heart of the biochemical apparatus responsible for coordinating this synthesis is the ribosome[1] – a macromolecular ensemble composed of both ribonucleic acid (RNA) and protein – and within the ribosome the key site of synthetic chemical interest is the peptidyl transferase centre (PTC).[2] It is here that peptide bonds are forged, via the sequential cross aminolysis of nucleophilic 3'-aminoacyl-tRNA esters and electrophilic 3'-*N*-acyl-aminoacyl-tRNA (peptidyl-tRNA) esters,[3] and here where peptides are eventually released by the hydrolysis of the final peptidyl-tRNA ester (Figure 1). The secondary structure and primary sequence of the RNA surrounding the PTC appears to be highly conserved across every kingdom of life, and this, combined with suggestive symmetry and the absence of ribosomal protein in the immediate vicinity of the PTC, has led to the suggestion that the RNA surrounding the PTC may constitute a vestige of a primordial transpeptidation ribozyme. The recent work of Yonath and co-workers,[4] demonstrating the possibility of peptide bond formation – albeit in trace amounts – mediated solely by fragments of this putative *protoribosome,*[4, 5, 6] provides notable support for this hypothesis.

Unlike typical protein-based *en*zymes, the catalytic competency of the ribosome is predicated on its ability to serve as an "entropy trap".[7-8] It catalyzes peptide synthesis not by enthalpic transition state stabilization, but by using the RNA surrounding the PTC to precisely align the two key substrates in a manner conducive to aminolysis, and by providing a desolvated environment in which passage through charge separated transition states (i.e., tetrahedral zwitterions) is not hampered by the need to reorganize solvent (water). Though unclear from existing data, it would seem reasonable to expect a similar *modus operandi* of a *proto*ribosome, given that parsimony supports the principle of continuity.[10]

The remarkable efficiency of ribosomal peptide synthesis, however, belies a significant problem for uncatalyzed or otherwise unassisted peptide synthesis under the same manifold: *in water, it simply isn't very good*. For example, even at highly elevated concentrations (400 mM), the auto-aminolysis of 2'(3')-*O*-(glycyl)-adenosine-5'-(*O*-methylphosphate) (MepA-Gly) in water – Orgel's chemical model for ribosomal peptide synthesis – is decidedly inefficient,[11a] with the combined yield of all peptide-derived products not surpassing 17% even under optimal conditions. MepA-Gly, an alkyl ester activated by virtue of aminoacyl *N*-protonation and by a competent diol leaving group, undergoes highly efficient hydrolysis around neutral pH;[9] it is this hydrolytic instability, combined with the

significant entropic barriers associated with direct aminolysis in water, that conspire to suppress the yield of peptide. Other chemical models of ribosomal peptide synthesis have encountered the same problem time and again:[11-13] for all but the most favourable or biased systems, outcompeting hydrolysis is hard, even at "the highest possible concentrations".[13]

Given the physical basis of ribosomal activity – encapsulation, desolvation, and mutual orientation of substrates – the woeful productivity of this chemistry in bulk aqueous solution would appear to pose an evolutionary dichotomy. On the one hand, one might conclude that the incipient stages of ribosomal peptide synthesis, based on the aminolysis of aminoacyl RNA esters, would have been too inefficient to convey any evolutionary advantage. In such a case, ribosomal peptide synthesis could only have emerged, somehow, *after* the independent development, for other reasons, of a ribozyme that fortuitously permitted the use of such substrates. An alternative conclusion might be that pre-ribosomal peptide synthesis relied on *fundamentally similar* chemistry – and similar substrates – to that now used in biology, but exploited some auxiliary mechanism, beyond *direct* amidation, to outcompete hydrolysis in the absence of ribozymatic assistance.

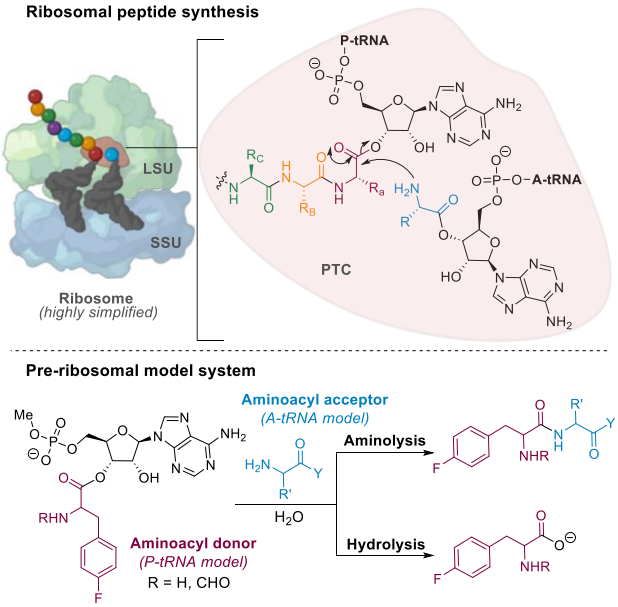

Figure 1. Underlying chemistry of ribosomal peptide synthesis

We were drawn to the second of these possibilities by the observations of Weber and Orgel,[11b] and the independent work of Jencks and co-workers.[14] Whilst the cross aminolysis of MepA-Gly (400 mM) with equimolar glycine (Gly) was shown to be just as inefficient as autoaminolysis, Orgel reported that a reaction with L-serine (Ser) exhibited a drastically different profile: not only did Gly-Ser, the cross-aminolysis product, form efficiently, but its formation even outpaced MepA-Gly hydrolysis under the particular conditions studied. This finding, combined with Jencks' observation of the enhanced nucleophilicity of serinyl hydroxyl groups,[14] points to the existence of a more efficient, *indirect* mechanism for peptide formation proceeding *via* transesterification to the serine hydroxyl group and *O*-to-*N* rearrangement (cf. native chemical ligation),[15] and thereby an opportunity for outcompeting hydrolysis in a pre-ribosomal world. The proven capacity of the extant ribosome to facilitate transesterification with α-hydroxy analogues of aminoacyl tRNA esters,[8, 16] our finding that serine and threonine (but not cysteine) precursors emerge naturally, as part of a limited subset of amino acids, from the cyanosulfidic reaction network,[17] and the reality that even the most fruitful demonstrations of *protoribosomal* activity have furnished little more than trace peptidation with *non-hydroxylated* aminoacyl acceptors,[4] all suggest this mechanism could have evolutionary significance hitherto underappreciated.

On this basis, and in light of the conflicting mechanisms proposed in the literature for such processes, we have sought to investigate, systematically and in quantitative detail, a *chemical model* system for ribosomal peptide formation. Our biomimetic system, designed to be amenable to *in situ* monitoring by ^{1}H-decoupled ^{19}F NMR spectroscopy (^{19}F{^{1}H}$_{IG}$ NMR), encompasses a range of ^{19}F-tagged aminoacyl adenylate esters as aminoacyl donors (P-tRNA analogues), differing in their degree of acylation, *N*-functionalisation, and stereochemistry, as well as a range of hydroxyl-bearing amino acid derivatives – plus non-hydroxylated controls – as aminoacyl acceptors (A-tRNA analogues). Herein we report the results of our investigation, and discuss the possible evolutionary implications of a pre-ribosomal dependence on *indirect* amidation.

Our study places earlier observations into an overarching framework; offers direct spectroscopic evidence and kinetic characterisation of the elusive serinyl ester intermediate; resolves apparent incongruities between the related conclusions of Pinck and Schuber,[18, 19] Orgel and Weber,[11] Wolfenden and co-workers,[7] and others;[20, 21] and offers subtle mechanistic insights from studies of concentration-, pH- and temperature-dependence. We also discuss possible functions for the hydroxyl-functionalised peptides – or lack thereof – that one would presumably expect to emerge from a dependence on *indirect* amidation in a pre-ribosomal world.

RESULTS

Preliminary Experiments

Preliminary work focused on the design of a chemical model system for ribosomal peptide formation that was readily amenable to *in situ* monitoring under a wide range of temperatures and conditions, and which represented a reasonable compromise between synthetic accessibility and fidelity to the conserved CCA-3' terminus of extant aminoacyl-tRNAs. Drawing on the substrates used in previous studies,[4, 7, 12, 13, 22, 23] we thus prepared 2'(3')-*O*-(4-fluoro-L-phenylalanyl)-adenosine-5'-(*O*-methylphosphate) (**MepA-L-PheF**) by conventional synthesis, with an eye to deploying ^{19}F{^{1}H}$_{IG}$ NMR for *in situ* monitoring.[24] Initial experiments focused on **MepA-L-PheF** rather than any *N*-acylated derivatives, both out of practical expediency and a desire to establish a benchmark for assessing the perturbation brought about by *N*-acylation. The pure monoester

MepA-L-PheF was isolated as a mixture of the 2'- and 3'-regioisomers by preparative reverse-phase HPLC (formic acid/acetonitrile; pH = 2.4) and lyophilization, and its identity confirmed by standard NMR characterization and LC/ESI(+)-MS (m/z = 527.0 g mol^{-1}; calc. 527.1 g mol^{-1}). Preliminary $^{19}F\{^1H\}_{IG}$ NMR monitoring of **MepA-L-PheF** (4 mM) in D_2O (pH* = 7.0; 20 °C) over time revealed two well-resolved, decaying singlets for the 2'- and 3'-regioisomers ($\Delta\delta_F \approx 200$ Hz), as well as a third, growing singlet attributed to, and subsequently confirmed as, 4-fluoro-L-phenylalanine (**L-PheF-OH**). As expected, the ratio of the two regioisomers remained constant at 65:35 (3':2'; $f_{\{Em,3'\}}$ = 65 %)[12, 25, 26] throughout the course of hydrolysis, indicating that 2',3'-aminoacyl exchange is rapid with respect to substrate hydrolysis but slow relative to $\Delta\delta_F$.[25]

To gauge the coarse efficiency of peptide formation in water with **MepA-L-PheF** as an aminoacyl donor, a range of independent reactions of **MepA-L-PheF** (2 mM)[27] and various aminoacyl acceptors were run under buffered conditions in D_2O (20°C). The aminoacyl acceptors, either achiral or single enantiomers, were used in large excess (600 mM), and their nucleophilic forms liberated with an appropriate amount of KOD to establish a buffer near the relevant pK_a*. Under these conditions, and as per Orgel's findings with **MepA-Gly**,[11b] quantitative *end-point* $^{19}F\{^1H\}_{IG}$ NMR analysis revealed minimal *cross*-aminolysis (yield < 5 %) with even the least hindered aminoacyl acceptors, including glycine (Gly-OH; pH*(20°C) = 10.3), glycinamide (Gly-NH_2; pH*(20°C) = 8.5) and L-alaninamide (L-Ala-NH_2; pH*(20°C) = 8.5). This was in stark contrast to the reactions with L-serine (L-Ser-OH; pH*(20°C) = 9.7; 42%), with L-serinamide (L-Ser-NH_2; pH*(20°C) = 7.7; 55%) and with L-serine *tert*-butyl ester (L-Ser-O^{t}Bu; pH*(20°C) = 7.7 ; 55 %), for which hydrolysis and aminolysis, strikingly, were almost *equally competitive* in each case. Significant, albeit lower, yields of amide were also observed following incubation with L-threoninamide (L-Thr-NH_2; pH*(20°C) = 7.4; 16 %), but only one product – that of hydrolysis – was observed in solutions buffered with *O*-methyl-L-serine (pH*(20°C) = 8.8) and *O*-phospho-L-serine (pH*(20°C) = 9.8) (both *O*-blocked). Notably, incubation of **MepA-L-PheF** with a mixture of *N*-acetyl-L-serine (600 mM; *N*-blocked) and buffering glycinamide (100 mM; pH*(20°C) = 7.6) also yielded significant quantities (27%) of a second product beyond L-PheF-OH, which on the basis of its hydrolytic lability at higher pH (pH*(20°C) > 9.5) was assigned as the transesterification product, *O*-(4-fluoro-L-phenylalanyl)-*N*-acetyl-L-serine.

Subtle modulations in these selectivities were observed with various derivatives of **MepA-L-PheF**, all synthesised and incubated in an analogous manner, with a subset of aminoacyl acceptors (see SI). Compared to **MepA-L-PheF**, modest increases in the apparent predisposition to amidation, all other things being equal, were observed in the case of 2'(3')-*O*-(*N*-formyl-4-fluoro-L-phenylalanyl)-adenosine-5'-(*O*-methylphosphate) (**MepA-*N*-f-L-PheF**), 2',3'-bis-*O*-(4-fluoro-L-phenylalanyl)-adenosine-5'-(*O*-methylphosphate) (**MepA-L-(PheF)$_2$**) and with D-serine *versus* L-serine, as well as at lower temperatures; similarly minor *reductions* in selectivity for aminolysis were observed with the diastereomeric aminoacyl donor **MepA-D-PheF**.

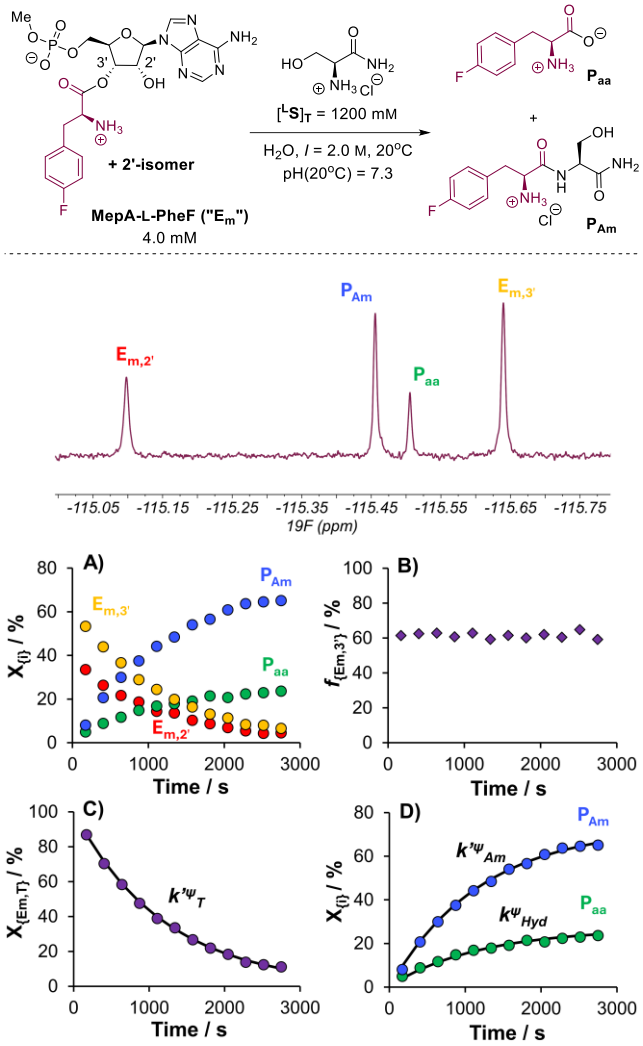

Figure 2. Chemical scheme, example $^{19}F\{^1H\}_{IG}$ NMR spectrum (376 MHz), and key temporal evolution profiles from the monitoring of a typical aminolysis of **MepA-L-PheF** (**Em**) with L-serinamide **LS** in aqueous solution (this example: H_2O, 20°C, pH = 7.3, *I* = 2.0 M). (A) Temporal evolution of experimental mole fractions of **Em,2'**, **Em,3'**, **PAm**, and **Paa**. (B) Temporal evolution of experimentally observed 2'/3' speciation of **Em**, with $f_{\{Em,3'\}}$ = [**Em,3'**]/[**Em**]$_T$ = fractional population of the 3'-isomer of **Em** over all charge states. (C) Temporal evolution of the mole fraction of **Em,T** with fit to kinetic model: **Em,T** → **PAm** (k^{ψ}_{Am}), **Em,T** → **Paa** (k^{ψ}_{Hyd}). (D) Temporal evolution of the mole fractions of **PAm** and **Paa** with fit to the kinetic model above. [**Em**]$_T$ = [**Em,2'**] + [**Em,3'**] = total concentration of **Em** in all charge states. k^{ψ}_T = *total pseudo first-order* rate constant for the decay of **Em,T**. $k^{\psi}_{Am} = f_{\{Am\}}.k^{\psi}_T = k'_{Am}.[\mathbf{LS}]_T$ = *pseudo first-order* rate constant for the *aminolysis* of **Em,T**. k'_{Am} = total *second-order* rate constant for the *aminolysis* of **Em,T**. $k^{\psi}_{Hyd} = f_{\{Hyd\}}.k^{\psi}_T$ = *pseudo first-order* rate constant for the *hydrolysis* of **Em,T**. [**Em,3'**] = [**Em,3'$^{(0)}$**] + [**Em,3'$^{(+)}$**], where [**Em,j'$^{(i)}$**] = concentration of j'-regioisomer with a charge of *i* on the α-amino group. $X_{\{i\}}$ = mole fraction of species i.

Kinetic Studies

Clearly, the presence – or absence – of an α-hydroxymethyl substituent in the aminoacyl acceptor exerts a profound effect on the efficiency of amide bond formation – and the ability of such acceptors to compete as nucleophiles with water. This observation would appear to implicate a distinct, indirect mechanism for aminolysis, comprising *O*-aminoacylation followed by intramolecular *O*-to-*N* rearrangement, yet various studies of similar systems[18, 21] have discounted such a pathway.

With this ambiguity in mind, we thus decided to set out on a detailed kinetic study of the aminolysis of **MepA-L-PheF** (hereafter "$\mathbf{E_m}$"; $[\mathbf{E_m}]_{T,0}$ = 4.0 mM) – and some key derivatives – using L-serinamide ($^{L}\mathbf{S}$) as a hydrolytically stable aminoacyl acceptor analogue.[28] All reactions were monitored *in situ* by $^{19}F\{^1H\}_{IG}$ NMR under pseudo-first order conditions, using a minimum of a 150-fold excess of *total* L-serinamide, $[^{L}\mathbf{S}]_T$, and the ionic strength of all reactions was standardised to 2.0 M using KCl as an inert salt.[29a] Free base L-serinamide, $^{L}\mathbf{S^0}$, was liberated from its hydrochloride salt *via* the addition of variable amounts of either KOH or KOD, depending upon whether aminolysis was monitored in H_2O or D_2O, and in all cases sufficient base was used to ensure that the pH (H_2O) or apparent pH* (D_2O) varied by < 0.1 units over the course of the reaction.[29b] $^{19}F\{^1H\}_{IG}$ NMR spectra were acquired identically in all cases, using parameters that allowed the relative quantitation of all key species to within < 5%, and all reactions were monitored to a minimum substrate conversion of 75% (i.e., two half-lives).

Under near neutral and moderately alkaline conditions, (pH*(20°C) ≈ 6.5 – 9.2), we found that the mono-exponential decay of the aminoacyl-monoester $\mathbf{E_m}$ was accompanied by the parallel, mono-exponential formation of two stable products (Figure 2): **L-PheF-OH** ("$\mathbf{P_{aa}}$"), the result of substrate hydrolysis, and *N*-(4-fluoro-L-phenylalanyl)-L-serinamide ($\mathbf{P_{Am}}$), the amide product. This is consistent with the observation of Wolfenden and others in related systems.[7,13] A typical set of reaction profiles is shown in Figure 2, alongside an example $^{19}F\{^1H\}_{IG}$ NMR spectrum acquired during *in situ* monitoring. No systematic drift was observed in the 2'/3' speciation of the monoester, $f_{\{Em,3'\}}$, in this example or within any other run, and therefore *pseudo* ("ψ") first-order rate constants (generally, k^{ψ}) for hydrolysis (k^{ψ}_{Hyd}) and aminolysis (k^{ψ}_{Am}) were determined by fitting the experimental mole fractions[29c] of the *total* monoester (2' + 3'), $\mathbf{E_{m,T}}$, as well as $\mathbf{P_{aa}}$ and $\mathbf{P_{Am}}$ to the equations:

$$X_{\{\mathbf{E_{m,T}}\}} = X_{\{\mathbf{E_{m,2'}}\}} + X_{\{\mathbf{E_{m,3'}}\}} = e^{-k_T^{\psi}t} \quad (1)$$

$$X_{\{\mathbf{P_{Am}}\}} = f_{\{Am\}}\left(1 - e^{-k_T^{\psi}t}\right) = \frac{k_{Am}^{\psi}}{k_T^{\psi}}\left(1 - e^{-k_T^{\psi}t}\right) \quad (2)$$

$$X_{\{\mathbf{P_{aa}}\}} = f_{\{Hyd\}}\left(1 - e^{-k_T^{\psi}t}\right) = \frac{k_{Hyd}^{\psi}}{k_T^{\psi}}\left(1 - e^{-k_T^{\psi}t}\right) \quad (3)$$

$$k_T^{\psi} = k_{Am}^{\psi} + k_{Hyd}^{\psi} \quad (4)$$

More complex reaction profiles were observed under mildly acidic conditions (pH* < 6.5), with the emergence of an intermediate species and subtly sinusoidal behaviour in the temporal evolution of the aminolysis product $\mathbf{P_{Am}}$ (Figure 3). The detection of the intermediate under such conditions was reproducible across different batches of $\mathbf{E_m}$, in H_2O and D_2O, and at different temperatures, *vide infra*, and global fitting of experimental populations to an analytical kinetic model (equations (2), (3), (5), (6)) in which the intermediate derives from $\mathbf{E_m}$ and decomposes to $\mathbf{P_{Am}}$ gave materially improved kinetic fits relative to a one-step model.

$$X_{\{\mathbf{I_{Es}}\}} = \left(\frac{k_{Am}^{\psi}}{k_r^{\psi} - k_T^{\psi}}\right)\left(e^{-k_T^{\psi}t} - e^{-k_r^{\psi}t}\right) \quad (5)$$

$$X_{\{\mathbf{P_{Am}}\}} = \frac{k_{Am}^{\psi}}{k_T^{\psi}}\left\{1 + \left(\frac{1}{k_r^{\psi} - k_T^{\psi}}\right)\left(k_T^{\psi}\, e^{-k_r^{\psi}t} - k_r^{\psi} e^{-k_T^{\psi}t}\right)\right\} \quad (6)$$

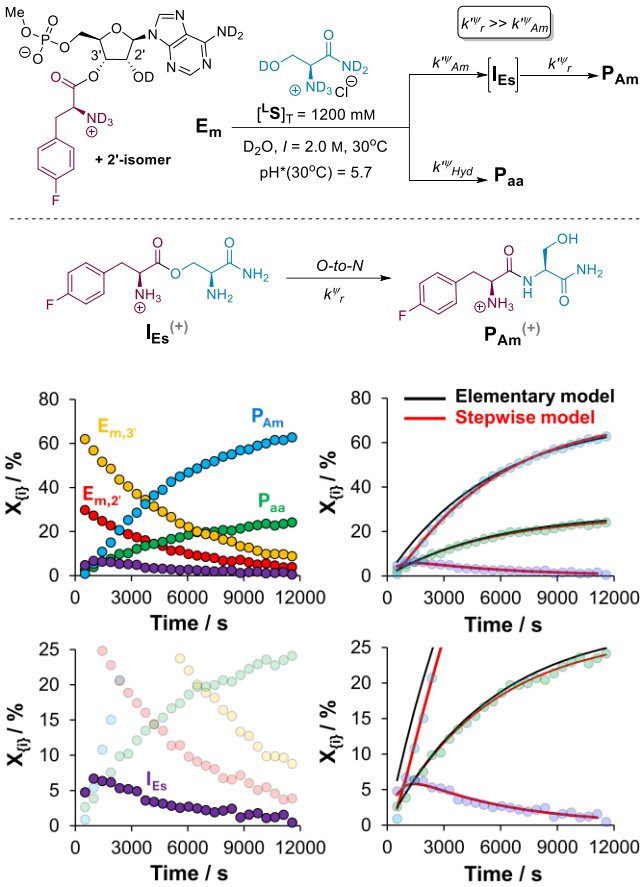

Figure 3. Kinetic scheme, temporal evolution profiles, and comparative fits to two distinct kinetic models for key species in a typical aminolysis of **MepA-L-PheF** ($\mathbf{E_m}$) with L-serinamide under a low pH regime (this example: D_2O, 30°C, pH*(30°C) = 5.7 , I = 2.0 M). Elementary model = $\mathbf{E_{m,T}} \rightarrow \mathbf{P_{Am}}$ (k^{ψ}_{Am}), $\mathbf{E_{m,T}} \rightarrow \mathbf{P_{aa}}$ (k^{ψ}_{Hyd}). Stepwise model: = $\mathbf{E_{m,T}} \rightarrow \mathbf{I_{Es}}$ (k^{ψ}_{Am}), $\mathbf{I_{Es}} \rightarrow \mathbf{P_{Am}}$ (k^{ψ}_{r}), $\mathbf{E_{m,T}} \rightarrow \mathbf{P_{aa}}$ (k^{ψ}_{Hyd}).

The kinetically implied provenance, and fate, of the intermediate, its greater accumulation at lower pH, and the relative stability of the transesterification product of $\mathbf{E_m}$ and *N*-acetyl-L-serine at pH*(20°C) ≈ 7.5, *vide supra*, lead

us to assign this species as the previously elusive serinyl ester intermediate, in this case *O*-(4-fluoro-L-phenylalanyl)-L-serinamide (**I_{Es}**).

Under the assumption of this assignment, the rate-determining step in the aminolysis **E_m** with L-serinamide must be interpreted as being *O-acylation*, such that the pseudo first-order rate constant k^{ψ}_{Am} actually reflects the rate of the initial *transesterification*; $k^{\psi}_{r,}$ measurable only at sufficiently low pH, then reflects the rate of the relatively rapid, intramolecular *O*-to-*N* rearrangement. This assignment is consistent with many,[20, 30] though not all,[18, 21] studies of the reactions of tris(hydroxymethyl)aminomethane (**Tris**) with various activated esters; it is also strongly indicated by the studies of Hansen,[31] and Porter and co-workers,[32] on the intramolecular *O*-to-*N* rearrangement of *O*-acetyl-ethanolamine in aqueous solution, and that of Phillips and Baltzly on the rearrangement of analogous esters of ethanolamine.[33]

With a means of monitoring and analytical kinetic deconvolution in place, the aminolysis – and concurrent hydrolysis – of **E_m** with L-serinamide in D_2O (20°C) was next studied systematically across the range pH*(20°C) = 6.0 – 9.3 (I = 2.0 M) (Figure 4). Two series of reactions – with different *total* L-serinamide concentrations $[^{L}\mathbf{S}]_T$ = 600 mM or 1200 mM – were conducted, with the pH* of each reaction adjusted by the addition of variable quantities of KOD to L-serinamide deuterochloride. The resultant pH*-rate profiles (pH*-k'_{Am}, pH*-k^{ψ}_{Hyd}; $k'_{Am} = k^{\psi}_{Am}/[^{L}\mathbf{S}]_T$), are shown in Figure 4. In accordance with Wolfenden's study with **Tris**[7a] – but in contrast to a second study with glycinamide[7b] – the fact that data from *both* series of experiments fall on the *same profiles* suggests that: (i) the rate of transesterification, and therefore overall aminolysis, is *first-order* with respect to $[^{L}\mathbf{S}]_T$; and (ii) the rate of hydrolysis is independent of $[^{L}\mathbf{S}]_T$. This appears to rule out significant general-base catalysis by L-serinamide, of either transesterification or hydrolysis, under these conditions.[34]

A satisfactory fit of the pH*-k'_{Am} profile was obtained by assuming that k'_{Am} comprises only two terms, including rates for: (i) the transesterification (formal aminolysis) of the aminoacyl ester (**E_m**) in its *N*-protonated state, **E_m^+** ($k_{Am,+}$); and (ii) the transesterification (formal aminolysis) of the free base aminoacyl ester, **E_m^0** ($k_{Am,0}$). It did not seem necessary to include any additional terms for, e.g., the specific-base catalysed reaction of L-serinamide with either **E_m^0** or **E_m^+**.[35] The second-order rate constants $k_{Am,+}$ and $k_{Am,0}$ are weighted averages of the corresponding constants for the 2' and 3'-regioisomers, since $[\mathbf{E_m}^i] = [\mathbf{E_{m,2'}}^i] + [\mathbf{E_{m,3'}}^i]$ (i = 0 or +). Assuming that only the free base state of L-serinamide, **$^{L}S^0$**, can undergo amidation, this means that:

$$\frac{d[\mathbf{P_{Am}}]}{dt} = \left(k_{Am,0}[\mathbf{E_m^0}] + k_{Am,+}[\mathbf{E_m^+}]\right)[^{L}\mathbf{S^0}] = k^{\psi}_{Am}[\mathbf{E_m}]_T \qquad (7)$$

$$k'_{Am} = \frac{k^{\psi}_{Am}}{[^{L}\mathbf{S}]_T} = \frac{k_{Am,0} + k_{Am,+}10^{\Delta pK_a^*(\mathbf{E_m^+})}}{\left(1 + 10^{\Delta pK_a^*(^{L}\mathbf{S^+})}\right)\left(1 + 10^{\Delta pK_a^*(\mathbf{E_m^+})}\right)} \qquad (8)$$

$$\Delta pK_a^*(X) = pK_a^*(\mathrm{X}) - pH^* \qquad (9)$$

The underlying second-order kinetic parameters, $k_{Am,+}$ and $k_{Am,0}$, and the apparent pK_a* of **E_m^+** were determined[36] by non-linear fitting (unweighted)[37a-b] of k^{ψ}_{Am} to equation 9, with the apparent pK_{aH}^* of L-serinamide, **^{L}S**, measured independently by $^{13}C\{^1H\}$ NMR titration under equivalent conditions (D_2O, 20 °C, I = 2.0 M), constrained during fitting (pK_{aH}^*(**^{L}S**; 20°C) = 7.94).

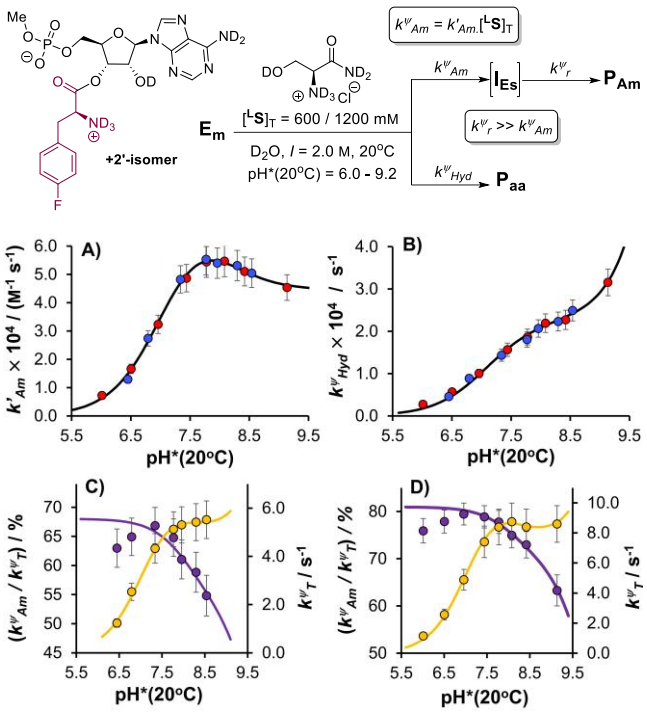

Figure 4. Kinetic analysis of the aminolysis of **E_m** with L-serinamide **^{L}S**, and concurrent hydrolysis, over the range pH* = 5.7 – 9.3 (20°C, D_2O, I = 2.0 M, KCl; $[\mathbf{E_m}]_{T,0}$ = 4.0 mM). (A) pH*-k'_{Am} profile for $[^{L}\mathbf{S}]_T$ = 600 mM (blue) and 1200 mM (red), with fit to experimental data. (B) pH*-k^{ψ}_{Hyd} profile, with same colour coding as (A), and fit to experimental data. (C) Empirical selectivity for aminolysis, $k^{\psi}_{Am}/k^{\psi}_{T}$, and total pseudo first-order rate of decay k^{ψ}_{T} as a function of pH*(20°C), with fits to experimental data, for $[^{L}\mathbf{S}]_T$ = 600 mM. (D) as for (C) but with $[^{L}\mathbf{S}]_T$ = 1200 mM. Fitted parameters ($k_{Am,+}$, $k_{Am,0}$, $k_{OH-,+}$, $k_{OH-,0}$; pK_a*(**E_m^+**) and their standard errors (Tables 1, S4) were determined by global, unweighted non-linear fitting of the pH*-k'_{Am} and pH*-k^{ψ}_{Hyd} profiles (*OriginPro 2024b*). Relative uncertainties in k^{ψ}_{Hyd} and k'_{Am} were conservatively estimated to be ± 10% (see SI). Uncertainties in k^{ψ}_{T} and $k^{\psi}_{Am}/k^{\psi}_{T}$ (not fitted directly) were calculated by propagation. See SI for further discussion.

An analogous process was followed for the pH*-k^{ψ}_{Hyd} profile, with two terms required to obtain a satisfactory fit to the experimental data, including rates for (L = H/D): (i) the *saponification* of **E_m^+** ($k_{OL-,+}$); and (ii) the *saponification* of **E_m^0** ($k_{OL-,0}$).[36,37] The underlying kinetic parameters were again determined by non-linear fitting (unweighted)[37a-b] to the appropriate equations, with the pK_a* of **E_m^+** obtained by *global fitting* of a common value to both the pH*-k'_{Am} and pH*-k^{ψ}_{Hyd} profiles.[38] The apparent self-ionisation constants of H_2O and D_2O, on the *molarity* scale, pK_w^*, were approximated from the thermodynamic values reported by Covington and co-workers,[39] with the activity coefficient

for the hydroxide/deuteroxide anion $\gamma_{OH^-} = \gamma_{OD^-} = 0.7$ approximated from Harned.[40]

$$\frac{d[\mathbf{P_{aa}}]}{dt} = \left(k_{OL^-,0}[\mathbf{E_m^0}] + k_{OL^-,+}[\mathbf{E_m^+}]\right)[\mathbf{OL^-}] = k^{\psi}_{Hyd}[\mathbf{E_m}]_T \quad (10)$$

$$k^{\psi}_{Hyd} = \frac{k_{OL^-,0} + k_{OL^-,+}10^{\Delta pK_a^*(\mathbf{E_m^+})}}{10^{\Delta pK_w^*}\left(1 + 10^{\Delta pK_a^*(\mathbf{E_m^+})}\right)} \quad (11)$$

$$\Delta pK_w^* = \log_{10}(\gamma_{OL}^-) + pK_w^* - pH^* \quad (12)$$

In coarse terms, the shape of the pH*-k^{ψ}_{Hyd} profile (Figure 4b) is consistent with that reported by Wolfenden for single-stranded leucyl-RNA,[9] and reflects the *combined influence* of pH* upon the *concentration* of hydroxide (with $[OH^-] \propto 10^{pH^*}$) and the *speciation* of $\mathbf{E_m}$ (Figure 5), as well as the different *reactivities* of $\mathbf{E_m^0}$ (i.e., $k_{OL^-,0}$) and $\mathbf{E_m^+}$ (i.e., $k_{OL^-,+}$). The factors governing the pH*-k'_{Am} profile (Figure 4a) are ultimately very similar, but the shape, featuring a *maximum* around pH*(20°C) ≈ 8, is clearly distinct. This arises from fact that the concentration of free base L-serinamide ($[\mathbf{^LS^0}]$) – the reactive nucleophile in aminolysis – saturates (i.e., $[\mathbf{^LS^0}] \rightarrow [\mathbf{^LS}]_T$) over the pH* range in Figure 4 in a way that the hydroxide concentration does not. Whilst increasing the pH* leads to *higher concentrations* of the active nucleophile in both reactions, it also shifts the speciation of the monoester towards its *less electrophilic* form, $\mathbf{E_m^0}$. The compensation of these two factors means that the changes in the *observed* rates of hydrolysis and aminolysis (Figure 4; k^{ψ}_{Hyd}, k'_{Am}) do not fully reflect, at least *visually,* the *intrinsic* reactivity differences of $\mathbf{E_m^0}$ and $\mathbf{E_m^+}$, thus requiring mathematical deconvolution.

The empirical *selectivity* for aminolysis, $k^{\psi}_{Am}/k^{\psi}_{T}$, is dependent on $[\mathbf{^LS}]_T$, but for both $[\mathbf{^LS}]_T$ = 600 mM and 1200 mM it appears to peak around pH*(20°C) ≈ 7.0 – 7.5. The significant drop in selectivity at *higher* pH* is a direct consequence of the saturation in $[\mathbf{^LS^0}]$, and this is captured fully by our analysis; the more subtle drop in selectivity at *lower* pH*, however, is not captured. We tentatively ascribe this to the (necessary)[37a] exclusion of the hydrolysis of $\mathbf{I_{Es}}$ to $\mathbf{P_{aa}}$ as a pathway from the underlying kinetic model (Figure 4, top). Such a pathway will be negligible above pH*(20°C) ≈ 7.5, but may become significant at lower pH* on account of the increasing degree of protonation of the α-amino group in $\mathbf{I_{Es}}$, which will simultaneously preclude *O*-to-*N* rearrangement and activate the intermediate to hydrolysis.[37b]

The *intrinsic reactivities* of $\mathbf{E_m^0}$ and $\mathbf{E_m^+}$ towards both aminolysis and hydrolysis, in the form of second-order rate constants, are summarised in Tables 1 and 2**.** A simple but important observation from this data pertains to the relative reactivities of water, hydroxide and free base L-serinamide towards $\mathbf{E_m^+}$: L-serinamide is six orders of magnitude *less reactive* than hydroxide, but at least four orders of magnitude *more reactive* than water itself ($k_{D2O,+} < 2 \times 10^{-7}$ M^{-1} s^{-1}; $[D_2O]$ = 55 M).[37c] Given that no kinetic term for the reaction of the L-serinamide alkoxide *anion* was required to reproduce the experimental pH*-k'_{Am} profile, this trend suggests that transesterification with *neutral* L-serinamide ought to involve intramolecular general base catalysis by its α-amino group,[20] though it cannot in itself give any indication as to the extent of proton transfer in the transition state. Some kind of qualitative constraint on this front may, though, be placed by noting that the protonation of the α-amino group in the *aminoacyl ester* accelerates saponification (e.g., $k_{OD^-,+}$ / $k_{OD^-,0}$ = 274; D_2O, 20°C) to a far *more significant* degree than transesterification (e.g., $k_{Am,+}$ / $k_{Am,0}$ = 13; D_2O, 20°C).[41] This in turn results in a precipitous drop in the *intrinsic* selectivity ($k_{OH^-,+}$ / $k_{Am,+}$ = 9.9 × 10^5; $k_{OH^-,0}$ / $k_{Am,0}$ = 4.7 × 10^4) for transesterification over saponification.[42] In the hypothetical limit of full intramolecular proton transfer in the transition state – i.e., if one imagines the reaction of the zwitterionic tautomer of L-serinamide – it might be expected that protonation of the aminoacyl ester would accelerate this reaction similarly to its reaction with hydroxide. That this is not observed suggests, in turn, that the charge distribution in the transition state for transesterification is quite distinct from saponification for either one, or both, of $\mathbf{E_m^0}$ or $\mathbf{E_m^+}$. Quantum chemical computations and hypothetical kinetic analysis appear to support this line of argument,[43a] but we cannot definitively rule out the direct reaction of the L-serinamide zwitterion in all contexts – especially in light of the dynamic subtleties that ought to be considered in distinguishing specific- and intramolecular general-base catalyzed processes.[43b]

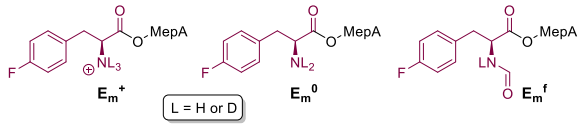

Figure 5. Simplified structural depictions of $\mathbf{E_m^+}$, $\mathbf{E_m^0}$ and the *N*-formylated derivative $\mathbf{E_m^f}$. Note that 2'-3' isomerization (not shown) appears to be limitingly rapid for both $\mathbf{E_m}$ and $\mathbf{E_m^f}$, relative to hydrolysis and aminolysis (pH* > 5.5), and so all rate constants and isotope effects in Tables 1 and 2 are weighted averages. See SI for details.

N-formylation of the aminoacyl ester[44] has an interesting effect: it accelerates saponification significantly, relative to $\mathbf{E_m^0}$, but modestly *suppresses* transesterification, with the upshot that the intrinsic selectivity for amide bond formation ($k_{OH^-,f}$ / $k_{Am,f}$ = 7.0 × 10^5) is very similar, though still superior, to the *protonated* ester, $\mathbf{E_m^+}$. That the intrinsic selectivity and hydrolytic lability of $\mathbf{E_m^f}$ is intermediate to $\mathbf{E_m^0}$ and $\mathbf{E_m^+}$ would appear to discount 5(4H)-oxazolones as intermediates in the transesterification and hydrolysis of the former, so the influence of *N*-formylation must represent a substituent perturbation on otherwise analogous transition states.[46]

Further pH*-k'_{Am} and pH*-k^{ψ}_{Hyd} profiles were subsequently measured in H_2O (20°C) and at two additional temperatures in D_2O (10°C, 30°C). These profiles (Figure 6) were analogous to those acquired in D_2O at 20°C, with all pH*-k^{ψ}_{Hyd} profiles exhibiting inflections around $pK_a(\mathbf{E_m^+})$, all pH*-k'_{Am} profiles exhibiting maxima around $pK_a(\mathbf{^LS^+})$, and the aminolysis selectivities deteriorating subtly at lower pH* in a manner not fully captured by our deconvolution.[37]

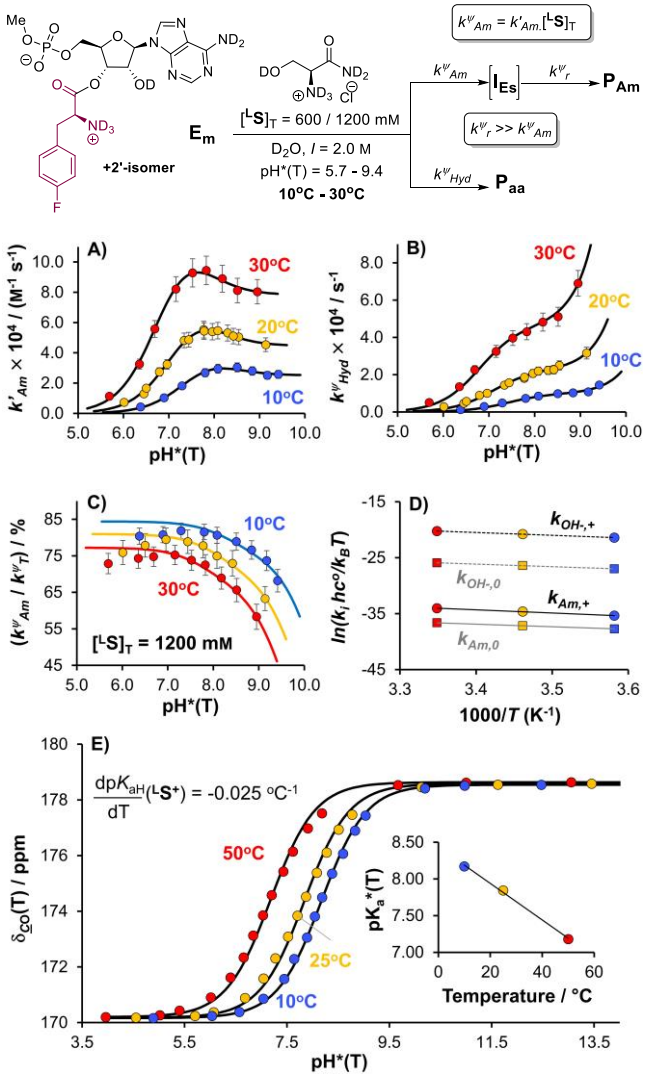

Figure 6. Temperature-dependence (10 – 30°C) of the hydrolysis and aminolysis of $\mathbf{E_m}$ with L-serinamide $^{L}\mathbf{S}$, as a function of pH* (D_2O, I = 2.0 M, KCl, $[\mathbf{E_m}]_{T,0} \approx 4$ mM). (A) Temperature dependence of the pH*-k'_{Am} profile (aminolysis), with (unweighted) fits to experimental data. (B) Temperature dependence of the pH*-k^{ψ}_{Hyd} profile (hydrolysis), with (unweighted) fits to experimental data. (C) Temperature and pH*-dependence of: (i) the empirical selectivity for aminolysis $k^{\psi}_{Am}/k^{\psi}_{T}$; and (ii) the total pseudo first-order rate of decay k^{ψ}_{T}, with fits to experimental data, for $[^{L}\mathbf{S}]_T$ = 1200 mM. (D) Linearised Eyring plots of the second-order rate constants $k_{Am,+}$, $k_{Am,0}$, $k_{OH-,+}$ and $k_{OH-,0}$. (E) $^{13}C\{^1H\}$ NMR titrations ($\delta_{13\underline{C}O}$) of L-serinamide (100 mM; D_2O, I = 2.0 M, KCl) at different temperatures ($[dpK_{aH}/dT]$ = -0.025 °C^{-1}; *cf* glycinamide[45]). pH*(10°C) = 6.38 – 9.42 (pK_a*($^{L}\mathbf{S}^+$) = 8.17). pH*(20°C) = 6.01 – 9.14 (pK_a*($^{L}\mathbf{S}^+$) = 7.94). pH*(30°C) = 5.69 – 8.95 (pK_a*($^{L}\mathbf{S}^+$) = 7.69). $[^{L}\mathbf{S}]_T$ = 600 – 2000 mM. Fitted parameters ($k_{Am,+}$, $k_{Am,0}$, $k_{OH-,+}$, $k_{OH-,0}$; pK_a*($\mathbf{E_m}^+$)) and their standard errors (Tables 1, S4) were determined by global, unweighted[37b] non-linear fitting of pH*-k'_{Am} and pH*-k^{ψ}_{Hyd} (*OriginPro 2024b*). See Figure 4 caption and SI for details of error analysis.

As before, the intrinsic reactivities of $\mathbf{E_m}^0$ and $\mathbf{E_m}^+$ towards aminolysis and hydrolysis, in the form of second-order rate constants, were extracted by non-linear fitting of the appropriate pH*-k^{ψ} profiles (Tables 1 and 2).

Table 1. Kinetic solvent isotope effects (k_H/k_D)$_i$ for the saponification and aminolysis of $\mathbf{E_m}$ with L-serinamide

i	k_i / (M^{-1} s^{-1}) ($\mathbf{H_2O}$)	k_i / (M^{-1} s^{-1}) ($\mathbf{D_2O}$)	(k_H/k_D)$_i$
Am, +	$4.6(3) \times 10^{-3}$	$5.8(2) \times 10^{-3}$	0.80(6)
Am, 0	$4.9(1) \times 10^{-4}$	$4.5(1) \times 10^{-4}$	1.10(3)
OL^-, +	$3.2(3) \times 10^{3}$	$5.7(2) \times 10^{3}$	0.56(6)
OL^-, 0	10(3)	21(2)	0.5(1)
Am, f	$4.1(2) \times 10^{-4}$	$3.3(2) \times 10^{-4}$	1.2(1)
OL-, f	$1.9(1) \times 10^{2}$	$2.3(1) \times 10^{2}$	0.83(4)

(k_H/k_D)$_i$ corresponds to the *solvent* (H_2O/D_2O) kinetic isotope effect (KIE) for the second-order rate constant k_i. Uncertainties in (k_H/k_D)$_i$ determined by propagation of standard errors in the individual rate constants k_i. All uncertainties and quoted in brackets (e.g., 1.0(2) = 1.0 ± 0.2). All KIEs measured at 20°C with I = 2.0 M (KCl).

For a given temperature and total loading of L-serinamide, the maximal yield of amidation, generally around pH$^{(*)}$ = p$K_a^{(*)}$($\mathbf{E_m}^+$), was found to increase slightly in D_2O (e.g., 20°C, $[^{L}\mathbf{S}]_T$ = 1.2 M: 80%;) compared to H_2O (75%). The data in Tables 1 and 2 suggest that this is the result of various underlying kinetic solvent isotope effects. Significant *inverse* solvent isotope effects were observed for the saponification of both the protonated ((k_H/k_D)$_{OL^-,+}$ = 0.56(6)) and free base ((k_H/k_D)$_{OL^-,0}$ = 0.5(1)) aminoacyl monoesters; an attenuated, but nevertheless still inverse, effect was also observed for the saponification of the *N*-formylated derivative ((k_H/k_D)$_{OH-,f}$ = 0.83(4)).[47] The value for the *N*-formyl-aminoacyl ester is highly typical of effects seen in the saponification of classic carboxylic esters,[48, 49] and may be the result of either rate-determining direct hydroxide attack or attack by water with general-base assistance by hydroxide.[50] The more inverse effects for the free aminoacyl ester, in either ionization state, must reflect an even more pronounced tightening of hydrogenic sites in the transition state;[51] though the basis for this is unclear, it is noteworthy that these values match closely the solvent effect observed for the specific-base catalyzed reaction of pentaerythritol with *p*-nitrophenyl acetate (k_H/k_D = 0.55).[21]

More interesting are the disparate solvent kinetic isotope effects observed for the transesterification of the free base, protonated, and *N*-formylated esters, with small *normal* effects observed for $\mathbf{E_m}^0$ and $\mathbf{E_m}^f$ but an *inverse* effect found for $\mathbf{E_m}^+$.[52] That the effects for $\mathbf{E_m}^+$ and $\mathbf{E_m}^0$ are so similar for saponification, but in opposite directions for transesterification, would appear to be diagnostic of some significant change in the nature of the transition state for transesterification in $\mathbf{E_m}^+$. One interpretation would be that the inverse effect for $\mathbf{E_m}^+$ reflects material alkoxide character in the transition state for transesterification, whilst the small normal effects for $\mathbf{E_m}^0$ and $\mathbf{E_m}^f$ reflect a transition state with less extensive O-H cleavage; this is understandable on the basis that greater alkoxide character in the L-serinamide hydroxyl group would benefit from both elec-

trostatic and hydrogen-bond stabilisation by an NH_3^+ substituent.

Table 2. Kinetic and acidity parameters for the aminolysis and hydrolysis of $\mathbf{E_m}$ with L-serinamide

	10°C	20°C	30°C
pK_a*(**LS^+**)	8.17(5)	7.94(5)	7.69(5)
(pK_a^D)	*(8.58(5))*	*(8.35(5))*	*(8.10(5))*
pK_a*(**E_m^+**)	7.40(5)	7.08(2)	6.79(3)
(pK_a^D)	*(7.81(5))*	*(7.49(2))*	*(7.20(3))*
pK_w*	15.03	14.64	14.29
(pK_w^D)	*(15.44)*	*(15.05)*	*(14.70)*
$k_{Am,+}$	$2.6(2) \times 10^{-3}$	$5.8(2) \times 10^{-3}$	$1.0(1) \times 10^{-2}$
$k_{Am,0}$	$2.5(1) \times 10^{-4}$	$4.5(1) \times 10^{-4}$	$7.8(1) \times 10^{-4}$
$k_{OL^-,+}$	$2.9(3) \times 10^{3}$	$5.7(2) \times 10^{3}$	$1.0(6) \times 10^{4}$
$k_{OL^-,0}$	11(3)	21(2)	35(3)
$k_{Am,f}$	-	$3.3(2) \times 10^{-4}$	$5.8(3) \times 10^{-4}$
$k_{OH^-,f}$	-	$2.3(1) \times 10^{2}$	$4.2(2) \times 10^{2}$

Second-order rate-constants (k; M^{-1} s^{-1}) and pK_a^*(**E_m^+**) values obtained by global non-linear fitting (unweighted)[37b] of experimental pH*-k'_{Am} and pH*-k^{ψ}_{Hyd} profiles (D_2O, I = 2.0 M) to equations 8 and 11; standard errors of fitted parameters determined with *OriginPro 2024b* unless otherwise stated and quoted in brackets (e.g., 1.0(2) = 1.0 ± 0.2). pK_a^*(**LS^+**) determined independently by $^{13}C\{^1H\}$ NMR titrations with estimated uncertainties of ± 0.05 units at all temperatures. All pK_a* values are apparent/empirical and not true thermodynamic values, with pD = pH* + 0.408.[7b] Apparent autoprotolysis constants in D_2O, pK_w*, were taken from Covington et al.[39] See SI for details.

The temperature dependence of the various kinetic parameters offers further insight. Higher temperatures, for example, appear to *enhance* the activating influence brought about by the protonation of the α-amino group in the *aminoacyl ester* – both $k_{Am,+}/k_{Am,0}$ and $k_{OH^-,+}/k_{OH^-,0}$ increase with temperature – but they tend to leave the intrinsic *selectivity* for transesterification (k_{OH^-}/k_{Am}) unaffected for all esters (**E_m^0**, **E_m^+**, **E_m^f**). Another key observation is that the activation parameters (Table 3) for the aminolysis of both **E_m^0** and **E_m^f** match almost quantitatively, in both their enthalpic-entropic partition and absolute values, those measured by Wolfenden for the reaction of **Tris** with the ethylene glycol ester of *N*-formyl glycine (**f-Gly-Glycol**).[7a] The correspondence of these activation parameters, the equivalent first-order dependence on nucleophile, and our *in situ* detection and kinetic characterization of **I_{Es}** with L-serinamide, all point to a unifying mechanism of rate-determining transesterification and rapid *O*-to-*N* rearrangement. This supports Orgel's hypothesis,[11b] and the findings of Jencks and Carriuolo[20] and de Jersey et al.[30] in related systems, but differs from the conclusions of Schuber and Pinck[18] and those of Bruice.[21] For both saponification and transesterification, protonation of the aminoacyl ester leads to significant *enthalpic destabilization* and a compensatory *entropic stabilization* of the transition state, with a net stabilization under ambient conditions.

Table 3. Transition state activation parameters for the aminolysis and hydrolysis of $\mathbf{E_m}$ and $\mathbf{E_m^f}$ with L-serinamide (D_2O, I = 2.0 M, 10 – 40 °C)

k_i / (M^{-1} s^{-1})	$\Delta^{\ddagger}H$ (kJ mol^{-1})	$\Delta^{\ddagger}S$ (J K^{-1} mol^{-1})	$-(T.\Delta^{\ddagger}S)_{293K}$ (kJ mol^{-1})	$\Delta^{\ddagger}G_{293K}$ (kJ mol^{-1})
$k_{Am,+}$	47 ± 4	-127 ± 12	37 ± 4	84 ± 5
$k_{Am,0}$	38 ± 1	-179 ± 2	52 ± 1	91 ± 1
$k_{OD^-,+}$	42 ± 1	-31 ± 3	9 ± 1	51 ± 1
$k_{OD^-,0}$	38 ± 1	-91 ± 4	27 ± 1	64 ± 2
$k_{Am,f}$	36 ± 2	-188 ± 6	55 ± 2	91 ± 3
$k_{OL^-,f}$	38 ± 1	-67 ± 4	20 ± 1	58 ± 2
k_{Tris}‡	38	-184	54	92
$k_{Gly\text{-}ND2}$†	33	-220	65	97

All activation parameters obtained by standard Eyring analysis, i.e., linear regression of $\ln(k_i hc°/k_B T)$ vs $1000/T$, with c° = 1 M. Standard errors in $\Delta^{\ddagger}H$ and $\Delta^{\ddagger}S$ (shown) were propagated to estimate the uncertainty in $\Delta^{\ddagger}G_{293K}$. ‡Wolfenden's study on the reaction of Tris with *N*-formyl-glycine glycol ester (f-Gly-Glycol). †A more recent study on the reaction of glycinamide (Gly-ND_2) with *N*-formyl-phenylalanine trifluoroethyl ester (f-Phe-TFE)

Inspired by the observations of Hecht on tandemly-activated tRNAs[23, 53] – their ability to serve as substrates in ribosomal synthesis, and their purportedly unusual stability to hydrolysis and aminolysis – we also studied the reaction of the *bis*-aminoacylated ester **MepA-(L-PheF)$_2$** (**E_{bis}**) with L-serinamide over the range pH* = 5.6 – 8.6 (D_2O, 20°C, I = 2.0 M). This species was invariably formed during our attempts to prepare **E_m**, by conventional synthesis, from **MepA** and equimolar **L-PheF-OH** (activated with CDI), suggesting that its formation is predisposed and thus of possible significance in the context of protoribosomal transpeptidation. All reactions, as before, were monitored over time by quantitative *in situ* $^{19}F\{^1H\}_{IG}$ NMR, and the kinetics deconvoluted by analytical means (see SI).

As anticipated, at sufficiently high pH* (> 6.5) the reaction of **E_{Bis}** with L-serinamide in aqueous solution affords **E_m** as an intermediate – with the expected equilibrium ratio of 2'- and 3'-isomers at any given pH* – and **P_{Am}** and **P_{aa}** as terminal products. These species were found to evolve, as expected, according to a simple kinetic scheme in which **E_{Bis}** and **E_m** undergo irreversible, (pseudo-)first order transformations to either **P_{Am}** (**E_{Bis}**: $k^{\psi}_{Am,Bis}$; **E_m**: k^{ψ}_{Am}) or **P_{aa}** (**E_{Bis}**: $k^{\psi}_{Hyd,Bis}$; **E_m**: k^{ψ}_{Hyd}). Reactions monitored at pH* < 6.5 led, again as anticipated, to the minor accumulation of the intermediate species **I_{Es}** (Figure 5), thus requiring the use of a more complex analytical model for kinetic deconvolution (Figure 7). The dipeptide **(L-PheF)$_2$**, which in principle could form from an intramolecular aminolysis *within* **E_{Bis}**,[54] was not detected under any conditions, in agreement with the findings of Hecht.[53]

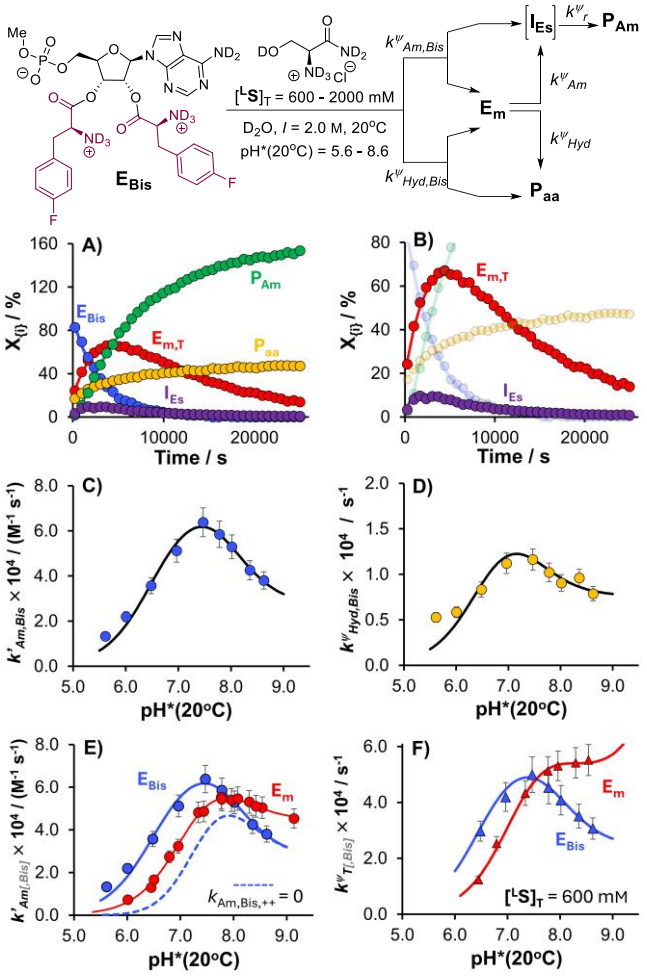

Figure 7. Example $^{19}F\{^1H\}_{IG}$ NMR monitoring data and kinetic analysis for the aminolysis, and concurrent hydrolysis, of **MepA-(L-PheF)$_2$** (**E$_{Bis}$**) with L-serinamide in D_2O (20 °C, pH* = 5.6 – 8.6, I = 2.0 M; $[^LS]_T$ = 600 – 2000 mM; $[E_{Bis}]_{T,0} \approx 4$ mM). (A) Temporal evolution profiles, with kinetic fits shown, for all key species under a low pH* regime (this example: pH* = 5.6, $[^LS]_T$ = 2000 mM). (B) Expanded view of (A), with a focus on the intermediate kinetics of **E$_{m,T}$** and **I$_{Es}$**. (C) pH*-$k'_{Am,Bis}$ profile with (unweighted) fit to experimental data ($k'_{Am,Bis} = k^{\psi}_{Am,Bis}/[^LS]_T$). (D) pH*-$k^{\psi}_{Hyd,Bis}$ profile with (unweighted) fit to experimental data. (E) Co-plot of the pH*-k'_{Am} (**E$_m$**) and pH*-$k'_{Am,Bis}$ (**E$_{Bis}$**) profiles; dotted line reflects pH*-$k'_{Am,Bis}$ profile without any contribution from the aminolysis of the doubly protonated state, **E$_{Bis}^{++}$** (i.e., $k_{Am,Bis,++} = 0$). (F) Co-plot of the pH*-k^{ψ}_T (**E$_m$**) and pH*-$k^{\psi}_{T,Bis}$ (**E$_{Bis}$**) profiles ($[^LS]_T$ = 600 mM). Kinetic model for pH* > 6.5 = **E$_{Bis}$** → **E$_{m,T}$** + **P$_{Am}$** ($k^{\psi}_{Am,Bis}$), **E$_{Bis}$** → **E$_{m,T}$** + **P$_{aa}$** ($k^{\psi}_{Hyd,Bis}$), **E$_{m,T}$** → **P$_{Am}$** (k^{ψ}_{Am}), **E$_{m,T}$** → **P$_{aa}$** (k^{ψ}_{Hyd}). Kinetic model for pH* < 6.5: = **E$_{Bis}$** → **E$_{m,T}$** + **I$_{Es}$** ($k^{\psi}_{Am,Bis}$), **E$_{Bis}$** → **E$_{m,T}$** + **P$_{aa}$** ($k^{\psi}_{Hyd,Bis}$), **E$_{m,T}$** → **I$_{Es}$** (k^{ψ}_{Am}), **E$_{m,T}$** → **P$_{aa}$** (k^{ψ}_{Hyd}), **I$_{Es}$** → **P$_{Am}$** (k^{ψ}_r). All steps are (pseudo; ψ) first-order. Fitted parameters ($k_{Am,Bis,++}$, $k_{Am,Bis,+}$, $k_{Am,Bis,0}$, $k_{OD\text{-},Bis,++}$, $k_{OD\text{-},Bis,+}$) and their standard errors in Table 4. pK_a*(**E$_{Bis}^{++}$**) and pK_a*(**E$_{Bis}^{+}$**) constrained during fitting; values taken from $^{19}F\{^1H\}$ NMR chemical shift analysis. See SI for details.

A satisfactory fit of the pH*-$k'_{Am,Bis}$ profile was obtained by assuming that $k'_{Am,Bis}$ comprises three terms, all featuring L-serinamide in its un-ionised state (**$^LS^0$**), including rates for the (formal) aminolysis of the bis-aminoacyl ester **E$_{Bis}$** in its: (i) *N*,*N*'-bis-protonated state, **E$_{Bis}^{++}$** ($k_{Am,Bis,++}$); (ii) *N*-monoprotonated state, **E$_{Bis}^{+}$** ($k_{Am,Bis,+}$); and (iii) doubly free base state, **E$_{Bis}^{0}$** ($k_{Am,Bis,0}$).[55] The pH*-$k^{\psi}_{Hyd,Bis}$ profile was deconvoluted in an analogous manner, by invoking separate terms for the saponification of **E$_{Bis}^{++}$** ($k_{OD\text{-},Bis,++}$), **E$_{Bis}^{+}$** ($k_{OD\text{-},Bis,+}$), and **E$_{Bis}^{0}$** ($k_{OD\text{-},Bis,0}$).[56] In each case, the intrinsic reactivities (second order rate constants) were obtained by non-linear fitting (unweighted) of the pH*-$k'_{Am,Bis}$ and pH*-$k^{\psi}_{Hyd,Bis}$ profiles (see SI for full analysis).[56] Given the more complex kinetic deconvolution (Figure 7, top) compared to reactions initiated with **E$_m$** (Figure 4), and given the more complex speciation of **E$_{Bis}$**, values for pK_a*(**E$_{Bis}^{++}$**) and pK_a*(**E$_{Bis}^{+}$**) were determined by $^{19}F\{^1H\}$ NMR chemical shift analysis (see SI) and constrained during fitting (Table 4).[57] The fits to both profiles are generally very good, with the expected outlier at pH*(20°C) = 5.6 likely the result of material partitioning of **I$_{Es}$** to **P$_{aa}$** (*vide supra*).[37]

Table 4. Kinetic and acidity parameters for the aminolysis and hydrolysis of E$_{Bis}$ with L-serinamide (20°C, D$_2$O, I = 2.0 M)

Species (X)	pK_a*(X)	k_{Am} / (M^{-1} s^{-1})	$k_{OD\text{-}}$ / (M^{-1} s^{-1})
E$_{Bis}^{++}$	6.43	0.011(1) †	1.0(1) × 10^{4}†
E$_{Bis}^{+}$	7.47	2.9(2) × 10^{-3}	8(2) × 10^{2}
E$_{Bis}^{0}$	-	1.3(2) ×10^{-4} †	n.d.
E$_m^{+}$	7.08(2)	5.8(2) × 10^{-3}	5.7(2) × 10^{3}
E$_m^{0}$	-	4.5(1) × 10^{-4}	21(2)

Second-order rate-constants (k; M^{-1} s^{-1}) obtained by non-linear fitting (unweighted)[37b] of experimental pH*-$k'_{Am,Bis}$ and pH*-$k^{\psi}_{Hyd,Bis}$ profiles (D_2O, I = 2.0 M) (see SI for equations); values for **E$_m$** taken directly from Table 2. Standard errors of second-order rate constants determined with *OriginPro 2024b* unless otherwise stated and quoted in brackets (e.g., 1.0(2) = 1.0 ± 0.2). pK_a*(**E$_{Bis}^{++}$**) and pK_a*(**E$_{Bis}^{+}$**) constrained during fitting; values taken from $^{19}F\{^1H\}$ NMR chemical shift analysis (see SI). †Rate constants "statistically" corrected for two (nearly) degenerate sites. See SI for details.

On a broad level, our second-order rate constants appear to be consistent with the empirical observations of Hecht and co-workers,[23] insomuch as the reactivity of the *neutral bis*-aminoacyl ester, **E$_{Bis}^{0}$**, is *notably suppressed* relative to the *neutral mono*-aminoacyl ester **E$_m^{0}$**. No saponification term for **E$_{Bis}^{0}$** could be established with sufficient confidence in the pH* range of our experiments, and the term for transesterification is, after statistical correction, roughly a quarter of that for **E$_m^{0}$**. The hydrolytic stability of **E$_m^{0}$** is particularly striking, and the main factor behind the divergence of the pH*-k^{ψ}_T and pH*-$k^{\psi}_{T,Bis}$ profiles (Figure 7F) at high pH*; though not measured directly,[58] the similarity between **E$_m^{0}$** and **E$_m^{f}$** (Table 2) would suggest that comparable stability ought to characterise the *N*-formylated derivative **E$_{Bis}^{f}$**.

A more nuanced trend emerges for the *monocationic* state of the *bis*-aminoacyl ester, **E$_{Bis}^{+}$**: it is much less reactive than **E$_m^{+}$** towards saponification, but only modestly less susceptible to transesterification with L-serinamide. A reasonable interpretation of this disparity may be that neighbouring group assistance from the vicinal 2'-OH

group plays a more significant role in saponification[49] than in transesterification;[7a] given the insensitivity of classical transition state probes[49] to such assistance, however, this conclusion must remain tentative. The statistically corrected reactivity of the *doubly protonated bis*-aminoacyl ester $\mathbf{E_{Bis}}^{++}$, meanwhile, is *enhanced* relative to $\mathbf{E_m}^+$, resulting in a crossover of the pH*-k'_{Am} and pH*-$k'_{Am,Bis}$ profiles, and in the *total* pseudo first-order decays of $\mathbf{E_m}$ and $\mathbf{E_{Bis}}$, around pH* = 7.5 (20°C, D_2O), I = 2.0 M). Thus, the bis-aminoacylated ester will, as previously observed, appear significantly more stable than the mono-aminoacyl ester – *but only at relatively high pH**.[59] This property has been correlated to the use of such bis-aminoacyl esters as ribosomal substrates in extreme thermophiles,[60] and in purely chemical terms it would appear to recommend their use as aminoacyl acceptors.

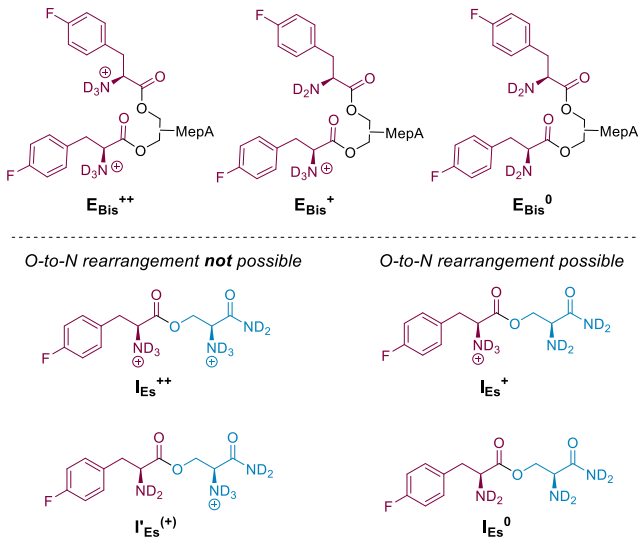

Figure 8. Structural depictions of $\mathbf{E_{Bis}}$ (simplified) and $\mathbf{I_{Es}}$ in their various charge states. Note that $[\mathbf{E_{Bis}}^+] = [\mathbf{E_{Bis,2'}}^+] + [\mathbf{E_{Bis,3'}}^+]$. For simplicity, we assume that $\mathbf{I_{Es}}^+$ and $\mathbf{I_{Es}}'^+$ have identical microscopic acidities.

Evolutionary implications and Conclusions

Ribosomal peptide synthesis in extant biology is remarkably efficient, and the underlying chemistry is shared by all known living systems. It is widely presumed to have underpinned the functioning of the Last Universal Common Ancestor (LUCA), but we know neither *how* this machinery emerged from chemistry, nor what selective pressure drove its emergence. The chemistry at the heart of ribosomal peptide formation – *direct* ester aminolysis – works well in the protective, desolvated environment of the peptidyl transferase centre (PTC) of the ribosome, but in bulk aqueous solution it is very inefficient. If, as imagined, ribosomal peptide synthesis is the consequence of the fortuitous emergence, and then extensive evolution, of some primordial transpeptidation ribozyme, the innate inefficiency of direct aminolysis in water would appear to pose a dichotomy for the origin of life.

Inspired by the previous observations of Orgel,[11] and of others,[7, 14, 18] we have therefore investigated an alternative, indirect manifold for pre-ribosomal peptide formation that instead proceeds *via* the formation of a serinyl intermediate ester and then *intra*molecular aminolysis via *O*-to-*N* rearrangement. We have explored this manifold by way of studies on a chemical model system, in which various 4-fluorophenylalanyl esters of adenosine-5'-(*O*-methylphosphate) serve as aminoacyl donor (P-tRNA) analogues and hydroxyl-functionalised amino acid derivatives serve as corresponding aminoacyl acceptor (A-tRNA) analogues. By the application of structure-reactivity relationships, *in situ* reaction monitoring by $^{19}F\{^1H\}_{IG}$ NMR, pH-rate profile analysis, and various transition state probes, we show, *inter alia*, that: (i) the competitive advantage provided by a hydroxymethyl/hydroxyethyl substituent in the aminoacyl acceptor is not only *profound*, but also *robust*, both with respect to structural modulations of the aminoacyl acceptor itself (e.g., serine esterification, amidation) and of the donor (e.g., *N*-formylation, bis-aminoacylation, 2'-deoxygenation); (ii) these substrates do, after all,[18,7a] react to afford serinyl *esters* as critical intermediates, but relatively rapid *O*-to-*N* rearrangement will generally preclude the discernible accumulation of such esters at or above neutral pH; (iii) at the concentrations needed to afford significant peptide bond formation, hydroxyl-functionalized aminoacyl acceptor analogues undergo rate-determining transesterification on a *bimolecular* basis, in contrast to *direct* aminolysis with non-hydroxylated acceptors, whose rates are typically dominated by formally *termolecular* terms, arising from the requirement for a distinct general base;[7b] (iv) the aminolysis of un-ionised, free aminoacyl esters appears to be kinetically similar and microscopically analogous to that of *N*-acyl-aminoacyl esters, allowing the use of *free* aminoacyl esters as P-tRNA analogues *at high pH**; (v) the α-hydroxymethyl group of L-serine, or analogues thereof, is boosted by *intra*molecular general base catalysis from the vicinal amino group, but it still retains significant nucleophilicity– albeit for different reasons[14] – if this amino group is acylated; and (vi) bis-aminoacyl esters appear to be considerably more stable to the corresponding mono-aminoacyl esters, with the exception of *free* bis-aminoacyl esters in their doubly protonated state.

Extant biology exploits various facets of simple chemistry to make ribosomal translation work – the initiation of translation with *N*-formyl methionine, for example, prevents the self-destruction of dipeptidyl-tRNAs by cyclisation to form diketopiperazines – and it occurs to us that several of the mechanistic features of *indirect* peptidation could have been useful in the evolution of (pre-)ribosomal peptide synthesis. At the broadest level, the ability of indirect peptidation to compete with hydrolysis at relatively modest concentrations of aminoacyl acceptor (10 – 100 mM, rather than > 1 M), without any catalysis, encapsulation or templating, would clearly provide an "easier" starting point from which to discover a nascent transpeptidation ribozyme. Furthermore, the bimolecular kinetics of the indirect mechanism – apparently the result of *intra*molecular general base catalysis – also means that the uncatalyzed process will be less inhibited at higher dilution than direct aminolysis, typically dominated by *termolecular* kinetics.[7b] That hydroxymethyl-bearing amino acids retain significant nucleophilicity when *N*-acylated[15] is also sug-

gestive to us, as it means that the incorporation of such amino acids into peptides or peptidyl-RNAs, in contrast to the alkyl amino acids (e.g. Gly, Ala, Leu, Val), does not eliminate their essential character.

Given that substrate promiscuity is a hallmark of ribozymatic catalysis,[61] it thus seem credible to envision a scenario in which a nascent transpeptidation ribozyme (protoribosome) would first emerge to catalyst indirect amidation with specific, α-hydroxmethyl-functionalized substrates, only to evolve, eventually, to accommodate – and encapsulate – otherwise analogous substrates devoid of these specific substituents. This evolutionary trajectory appeals to us as: (i) it does not require evolution to supplant some completely different form of chemistry altogether in developing ribosomal translation; (ii) the initial, uncatalyzed chemistry relies on amino acids that emerge naturally from the cyanosulfidic reaction network of prebiotic chemistry;[17] and (iii) the ribosome in extant biology remains perfectly capable of effecting transesterification[16] as well as transpeptidation, consistent with the idea that evolution simply enabled the expansion of substrate scope.

It occurs to us that one might imagine two broadly distinguishable possibilities for the selective pressure that could have driven such an evolutionary trajectory for the ribosome. On the one hand, it may be imagined that the X-Ser peptides that ought to have initially predominated possessed some function that was directly selectable; in such a case, ribosomal evolution could have been driven by continuous selection for improvement of that function. It is not clear to us exactly what this function could have been, though an ability to furnish RNA, by complexation, with nucleophilic functionality might have been significant.[6, 62] Alternatively, it may have been that these X-Ser peptides had no function *per se*, in which case the selective pressure for ribosome evolution might have arisen from the *process* of their formation. In this respect we are intrigued by the idea that (proto-)ribosomal peptide synthesis evolved not to make peptides, but to deblock aminoacyl RNA in preparation for replication/ligation, i.e., that the product of real evolutionary value in pre-ribosomal peptide synthesis transpeptidation was the *free oligoribonucleotide* rather than the peptide. Again, the reactions of hydroxymethyl-bearing amino acids (e.g., serine) are particularly useful in this respect, as a significant degree of their nucleophilicity is preserved upon peptidation.[14]

Supporting Information

The Supporting Information is available free of charge on the ACS Publications website.

Synthetic procedures, compound characterization data (NMR, ESI-MS), methods for kinetic studies, mathematical derivations of kinetic models, details of pH-rate profile deconvolution, raw kinetic data, raw pH-rate profile data, summaries of all key rate coefficients (pdf)

AUTHOR INFORMATION

Corresponding Authors

John D. Sutherland – MRC Laboratory of Molecular Biology, Francis Crick Avenue, Cambridge Biomedical Campus, Cambridge, CB2 0QH, U.K.; Email: johns@mrc-lmb.cam.ac.uk

Harvey J. A. Dale – MRC Laboratory of Molecular Biology, Francis Crick Avenue, Cambridge Biomedical Campus, Cambridge, CB2 0QH, U.K.; Email: hdale@mrc-lmb.cam.ac.uk

Author Contributions

The manuscript was written through contributions of both authors.

Notes

The authors declare no competing financial interest.

ACKNOWLEDGMENT

This work is supported by the Medical Research Council MC_UP_A024_1009 (J.D.S.). Additional financial support in the form of Research Fellowships from the Royal Commission for the Exhibition of 1851 (H.J.A.D.) and Emmanuel College, Cambridge (H.J.A.D.) is gratefully acknowledged. We are grateful to a careful reviewer (anonymous) for their insightful comments on the partitioning of the intermediate $\mathbf{I_{ES}}$ and its likely pH* dependence.

ABBREVIATIONS

P-tRNA = peptidyl transfer ribonucleic acid
A-tRNA = aminoacyl (acceptor) transfer ribonucleic acid
PTC = peptidyl transferase centre

REFERENCES

(1) (a) Ban, N.; Nissen, P.; Hansen, J.; Moore, P. B.; Steitz, T. A. The Complete Atomic Structure of the Large Ribosomal Subunit at 2.4 Å Resolution. *Science* **2000**, *289*, 905-920. (b) Nissen, P.; Hansen, J.; Ban, N.; Moore, P. B.; Steitz, T. A. The Structural Basis of Ribosome Activity in Peptide Bond Synthesis. *Science* **2000**, *289*, 920-930. (c) Schlünzen, F.; Zarivach, R.; Harms, J.; Bashan, A.; Tocilj, A.; Albrecht, R.; Yonath, A.; Franceschi, F. Structural basis for the interaction of antibiotics with the peptidyl transferase centre in eubacteria. *Nature* **2001**, *413*, 814-821. (d) Harms, J.; Schluenzen, F.; Zarivach, R.; Bashan, A.; Gat, S.; Agmon, I.; Bartels, H.; Franceschi, F.; Yonath, A. High Resolution Structure of the Large Ribosomal Subunit from a Mesophilic Eubacterium. *Cell* **2001**, *107*, 679-688. (e) Hansen, J. L.; Schmeing, T. M.; Moore, P. B.; Steitz, T. A. Structural insights into peptide bond formation. *Proc. Natl. Acad. Sci. USA* **2002**, *99*, 11670-11675. (f) Beringer, M.; Bruell, C.; Xiong, L.; Pfister, P.; Bieling, P.; Katunin, V. I.; Mankin, A. S.; Böttger, E. C.; Rodnina, M. V. Essential Mechanisms in the Catalysis of Peptide Bond Formation on the Ribosome. *J. Biol. Chem.* **2005**, *280*, 36065-36072. (g) Trobro, S.; Åqvist, J. Mechanism of peptide bond synthesis on the ribosome. *Proc. Natl. Acad. Sci. USA* **2005**, *102*, 12395-12400. (h) Bowman, J. C.; Petrov, A. S.; Frenkel-Pinter, M.; Penev, P. I.; Williams, L. D. Root of the Tree:

The Significance, Evolution, and Origins of the Ribosome. *Chem. Rev.* **2020**, *120*, 4848-4878.
(2) (a) Polacek, N.; Mankin, A. S. The Ribosomal Peptidyl Transferase Center: Structure, Function, Evolution, Inhibition. *Crit. Rev. Biochem. Mol. Biol.* **2005**, *40*, 285-311. (b) Beringer, M.; Rodnina, M. V. The Ribosomal Peptidyl Transferase. *Mol. Cell* **2007**, *26*, 311-321.
(3) Huang, K. S.; Weinger, J. S.; Butler, E. B.; Strobel, S. A. Regiospecificity of the Peptidyl tRNA Ester within the Ribosomal P Site. *J. Am. Chem. Soc.* **2006**, *128*, 3108-3109.
(4) Bose, T.; Fridkin, G.; Davidovich, C.; Krupkin, M.; Dinger, N.; Falkovich, Alla H.; Peleg, Y.; Agmon, I.; Bashan, A.; Yonath, A. Origin of life: protoribosome forms peptide bonds and links RNA and protein dominated worlds. *Nucleic Acids Res.* **2022**, *50*, 1815-1828.
(5) (a) Noller, H. F. Ribosomal RNA and Translation. *Ann. Rev. Biochem.* **1991**, *60*, 191-227. (b) Green, R.; Noller, H. F. Ribosomes and Translation. *Ann. Rev. Biochem.* **1997**, *66*, 679-716. (c) Davidovich, C.; Belousoff, M.; Wekselman, I.; Shapira, T.; Krupkin, M.; Zimmerman, E.; Bashan, A.; Yonath, A. The Proto-Ribosome: An Ancient Nano-machine for Peptide Bond Formation. *Isr. J. Chem.* **2010**, *50*, 29-35.
(6) Noller, H. F. Evolution of Protein Synthesis from an RNA World. *Cold Spring Harb. Perspect. Biol.* **2012**, *4:a003681*
(7) (a) Sievers, A.; Beringer, M.; Rodnina, M. V.; Wolfenden, R. The ribosome as an entropy trap. *Proc. Natl. Acad. Sci. USA* **2004**, *101*, 7897-7901. (b) Schroeder, G. K.; Wolfenden, R. The Rate Enhancement Produced by the Ribosome: An Improved Model. *Biochemistry* **2007**, *46*, 4037-4044.
(8) Bieling, P.; Beringer, M.; Adio, S.; Rodnina, M. V. Peptide bond formation does not involve acid-base catalysis by ribosomal residues. *Nat. Struct. Mol. Biol.* **2006**, *13*, 423-428.
(9) Wolfenden, R. *Biochemistry* **1963**, *2*, 1090–1092.
(10) Orgel, L. E. Evolution of the genetic apparatus. *J. Mol. Biol.* **1968**, *38*, 381-393.
(11) (a) Weber, A. L.; Orgel, L. E. The formation of peptides from the 2′(3′)-glycyl ester of a nucleotide. *J. Mol. Evol.* **1978**, *11*, 189-198. (b) Weber, A. L.; Orgel, L. E. The formation of dipeptides from amino acids and the 2′(3′)-glycyl ester of an adenylate. *J. Mol. Evol.* **1979**, *13*, 185-191.
(12) Hiller, D. A.; Zhong, M.; Singh, V.; Strobel, S. A. Transition States of Uncatalyzed Hydrolysis and Aminolysis Reactions of a Ribosomal P-Site Substrate Determined by Kinetic Isotope Effects. *Biochemistry* **2010**, *49*, 3868-3878.
(13) Watts, R. E.; Forster, A. C. Chemical Models of Peptide Formation in Translation. *Biochemistry* **2010**, *49*, 2177-2185.
(14) Anderson, B. M.; Cordes, E. H.; Jencks, W. P. Reactivity and Catalysis in Reactions of the Serine Hydroxyl Group and of O-Acyl Serines. *J. Biol. Chem.* **1961**, *236*, 455-463.
(15) (a) Dawson, P. E.; Muir, T. W.; Clark-Lewis, I.; Kent, S. B. H. Synthesis of Proteins by Native Chemical Ligation. *Science.* **1994,** *266,* 776-779. (b) Agouridas, V.; El Mahdi, O.; Diemer, V.; Cargoët, M.; Monbaliu, J. M.; Melnyk, O. Native Chemical Ligation and Extended Methods: Mechanisms, Catalysis, Scope, and Limitations. *Chem. Rev.* **2019**, *119*, 7328–7443.
(16) Fahnestock, S.; Neumann, H.; Shashoua, V.; Rich, A. Ribosome-catalyzed ester formation. *Biochemistry* **1970**, *9*, 2477-2483.
(17) Patel, B. H.; Percivalle, C.; Ritson, D. J.; Duffy, C. D.; Sutherland, J. D. Common origins of RNA, protein and lipid precursors in a cyanosulfidic protometabolism. *Nat. Chem.* **2015**, *7*, 301-307.
(18) (a) Pinck, M.; Schuber, F. Reaction of tris-(hydroxymethyl)-aminomethane with valyl-TYMV-RNA. *Biochimie* **1971**, *53*, 887-891. (b) Schuber, F.; Pinck, M. On the chemical reactivity of aminoacyl-tRNA ester bond: II. Aminolysis by tris and diethanolamine. *Biochimie* **1974**, *56*, 391-395.
(19) Schuber, F.; Pinck, M. On the chemical reactivity of aminoacyl-tRNA ester bond: I - Influence of pH and nature of the acyl group on the rate of hydrolysis. *Biochimie* **1974**, *56*, 383-390.
(20) Jencks, W. P.; Carriuolo, J. Reactivity of Nucleophilic Reagents toward Esters. *J. Am. Chem. Soc.* **1960**, *82*, 1778-1786.
(21) Bruice, T. C.; York, J. L. The Mechanism of the Reaction of Tris-(hydroxymethyl)-aminomethane and Pentaerythritol with Phenyl Esters. *J. Am. Chem. Soc.* **1961**, *83*, 1382-1387.
(22) (a) Schmeing, T. M.; Seila, A. C.; Hansen, J. L.; Freeborn, B.; Soukup, J. K.; Scaringe, S. A.; Strobel, S. A.; Moore, P. B.; Steitz, T. A. A pre-translocational intermediate in protein synthesis observed in crystals of enzymatically active 50S subunits. *Nat. Struct. Mol. Biol* **2002**, *9*, 225-230. (b) Hiller, D. A.; Singh, V.; Zhong, M.; Strobel, S. A. A two-step chemical mechanism for ribosome-catalysed peptide bond formation. *Nature* **2011**, *476*, 236-239.
(23) Duca, M.; Trindle, C. O.; Hecht, S. M. Structural Basis for the Exceptional Stability of Bisaminoacylated Nucleotides and Transfer RNAs. *J. Am. Chem. Soc.* **2011**, *133*, 11368-11377.
(24) The alanyl monoester of 5'-AMP has been shown by Hecht [*J. Am. Chem. Soc.* **2011**, *133*, 11368-11377] to have very similar reactivity to larger dinucleotide analogues towards various nucleophiles, and model/fragment reactions used by Steitz [e.g., *Science* **2000**, *289*, 920-930], Wolfenden [e.g., *Biochemistry* **2007**, *46*, 4037-4044], Strobel [e.g., Nature **2011**, *476*, 236-239], and Yonath [e.g., *Nucleic Acids Res.* **2022**, *50*, 1815-1828], as well as others, have used P-tRNA analogues featuring a (modified) phenylalanine residues.
(25) Wolfenden, R.; Rammler, D. H.; Lipmann, F. On the Site of Esterification of Amino Acids to Soluble RNA. *Biochemistry* **1964**, *3*, 329-338.
(26) Griffin, B. E.; Jarman, M.; Reese, C. B.; Sulston, J. E.; Trentham, D. R. Some Observations Relating to Acyl Mobility in Aminoacyl Soluble Ribonucleic Acids. *Biochemistry* **1966**, *5*, 3638-3649.
(27) The self-aminolysis of **MepA-L-PheF** at such dilution is negligible.
(28) Using L-serinamide as an A-tRNA analogue as opposed to, e.g., the ethyl or ethylene glycol ester of L-serine, simplified matters by preventing hydrolysis of the nucleophilic fragment. This ensured that all reactions evolved under constant pH, and that the amide products were themselves stable, both to hydrolysis and 2,5-diketopiperazine formation, on the timescales of our kinetics experiments.
(29) (a) The ionic strength was standardised to $I \approx 2.0$ M across all kinetics experiments by adding sufficient KCl such that $[KCl]_0 + [^{L}S]_T = 2.0$ M, with L-serinamide added as its *hydrochloride salt* and $[KCl]_0$ corresponding to the nominal concentration arising from the addition of solid KCl alone (i.e., excluding the KCl generated in situ from the neutralisation of $^{L}\mathbf{S}^{+}.Cl^{-}$ by added KOH). All other components (< 10 mM) were neglected in the calculation of ionic strength. KCl was obtained in BioXtra grade (> 99.0 %) from Sigma Aldrich, with the following specifications: < 0.001% Mg; < 0.005% Ca; < 0.0005% Cu; < 0.0005% Zn. Control end-point experiments with either added: (i) MgCl2 (2 mM); (ii) EDTA (10 mM); or (iii) $MgCl_2$ (2 mM) + EDTA (10 mM) showed no effect on aminolysis selectivity relative to the absence of these additives for the reaction of $\mathbf{E_{Bis}}$ (2 mM; pH* = 7.4, 20 °C, D_2O, $I = 2.0$ M) (b) In this work, pH measurements made on H_2O solutions, using protiated calibrants and electrode filling solutions, are denoted 'pH'; measurements made on D_2O solutions using such calibrants and reference solutions are apparent values, denoted pH*. All pK_a values determined in D_2O for this work pertain to apparent values, pK_a*; the corrected pK_a^D values may be approximated from pK_a^D = pK_a* + 0.408. None of the acid dissociation constants determined in this work constitute strict thermodynamic values; they are all empirical values,

reflecting the high ionic strength conditions under which they were measured (I = 2.0 M). As all measurements were made in a self-consistent manner, these values were nevertheless useful for the calculation of acid/base speciation. (c) The mole fraction of a given species i was calculated from $X_i = (I_i / \Sigma I)$, where I_i = integral of ^{19}F resonance for species i and Σ I is the summation of integrals over all species.
(30) (a) de Jersey, J.; Zerner, B. Spontaneous and α-chymotrypsin-catalyzed hydrolysis of 4-cis-benzylidene-2-phenyloxazolin-5-one. Catalysis by tris(hydroxymethyl) aminomethane. *Biochemistry* **1969**, *8*, 1975-1983. (b) de Jersey, J.; Fihelly, A. K.; Zerner, B. On the mechanism of the reaction of tris(hydroxymethyl)aminomethane with activated carbonyl compounds: A model for the serine proteinases. *Bioorg. Chem. Chemistry* **1980**, *9*, 153-162.
(31) Hansen, B. Kinetics of the Reactions of O-Acetylethanolamine. *Acta Chem. Scand*. **1963**, 17, 1307-1314.
(32) Porter, G. R.; Rydon, H. N.; Schofield, J. A. Transformations of 2-methyl-Δ2-oxazoline in aqueous solution. *J. Chem. Soc.* **1960**, 2686-2690.
(33) Phillips, A. P.; Baltzly, R. Rearrangements between Primary Ethanolamides of Carboxylic Acids and the Corresponding Aminoethylesters*. *J. Am. Chem. Soc.* **1947**, *69*, 200-204.
(34) It does not, though, rule out general-base catalysis of the *O*-to-*N* rearrangement of $\mathbf{I_{Es}}$ by L-serinamide.
(35) Bruice [*J. Am. Chem. Soc.* **1961**, *83*, 1382-1387] identified such a term for the reaction of Tris with p-nitrophenyl acetate, but Jencks [*J. Am. Chem. Soc.* **1960**, *82*, 1778-1786] did not. We favour the simplest interpretation of our data, and so see no need to invoke Bruice's additional term for this system.
(36) The (kinetic) observed pK_a* of $\mathbf{E_m}^+$ is a weighted average of the independent pK_a* values of the 2'- and 3'-regioisomers, $\mathbf{E_{m,2'}}^+$ and $\mathbf{E_{m,3'}}^+$; a separate analysis of the total 2'/3' speciation, $f_{\{Em,3'\}}$, as a function of pH* suggests that $\mathbf{E_{m,2'}}^+$ is 0.2 – 0.3 units more acidic than $\mathbf{E_{m,3'}}^+$ (see SI for details). Similarly, the second-order rate constants are weighted averages of the corresponding constants for the 2'- and 3'-regioisomers; see SI for details of weighting.
(37) (a) The apparent deterioration in empirical selectivity for aminolysis below neutral pH* (ca. pH*(20°C) < 7.0), though modest in our range of experiments, suggests either: (i) the existence of an anomalously large term for the spontaneous (water) hydrolysis of $\mathbf{E_m}^+$ (or $\mathbf{E_{Bis}}^{++}$), or else (ii) a material partitioning of the intermediate $\mathbf{I_{Es}}$ to $\mathbf{P_{aa}}$, which otherwise appears to undergo near-quantitative *O*-to-*N* rearrangement above neutral pH* (as per, e.g., Hansen in *Acta Chem. Scand*. **1963**, 17, 1307-1314). Whilst likely to be useful in distinguishing these two possibilities, kinetics experiments exploring the reactivity of $\mathbf{E_m}^+$ and independently synthesised $\mathbf{I_{Es}}$ at pH*(20°C) < 5.5 were outside the scope of this work. For this reason, pH*-k^{ψ}_{Hyd} profiles were fitted with a minimal model, using saponification terms only, in line with the original deconvolution of Wolfenden [*Biochemistry* **1963**, *2*, 1090–1092]. In this respect we are grateful to a careful and insightful reviewer (anonymous), who encouraged us to reconsider our initial analysis favouring (i); we are now strongly inclined to favour (ii) as the primary reason for the apparent deterioration in aminolysis selectivity below neutral pH*. (b) In light of the conclusion above (37(a)), our underlying kinetic model, assuming quantitative *O*-to-*N* rearrangement of $\mathbf{I_{Es}}$, is likely to be decreasingly appropriate for solutions at lower pH*; it is on this basis that we opt to fit our pH*-k^{ψ} profiles in an *unweighted* fashion. Alternative fittings are summarised in the SI. (c) An upper bound for the spontaneous (water) hydrolysis of $\mathbf{E_m}^+$ was estimated by including such a term in fitting the pH*-k^{ψ}_{Hyd} profile.
(38) The apparent value for the pK_a*of $\mathbf{E_m}^+$ is very similar to the previously determined value phenylalanine methyl ester (pK_a(25°C) = 7.15; H_2O, I(NaCl) = 0.1) [*Can. J. Chem*. **1971**, *49*, 3468-3476].
(39) Covington, A. K.; Robinson, R. A.; Bates, R. G. The Ionization Constant of Deuterium Oxide from 5 to 50°. *J. Phys. Chem.* **1966**, *70*, 3820-3824.
(40) Harned, H. S. The Activity Coefficient of Potassium Hydroxide in Potassium Chloride Solutions. *J. Am. Chem. Soc.* **1925**, *47*, 689-692.
(41) The magnitude of the rate enhancement of saponification brought about by substrate protonation is consistent with Wolfenden's earlier study on the hydrolysis of L-leucyl-RNA ($k_{OH-,+}$ / $k_{OH-,0}$ = 170; 37 °C, H_2O, I(KCl) = 0.3 M [Biochemistry 1963, *2*, 1090–1092].
(42) Note that the high intrinsic selectivity of $\mathbf{E_m}^0$ for transesterification is not accessible in practice; only at very high pH (>10), significantly beyond the saturation of free L-serinamide, is the saponification of $\mathbf{E_m}^+$ superseded by that of $\mathbf{E_m}^0$ as the major hydrolytic pathway for $\mathbf{E_m}$.
(43) (a) Quantum chemical computations, with thermostatistical corrections, at the r2SCAN-3c/def2-mTZVPP/SMD(H_2O) level (CENSO) level and comparison to choline (pK_a = 13.9) suggests that the *microscopic pK_a for the O-H proton* in $\mathbf{^LS^+}$ is 13.0, and in turn that the L-serinamide zwitterion would have to be considerably more reactive than hydroxide towards $\mathbf{E_m}^0$ to account for the magnitude of $k_{Am,0}$. The same analysis applied to $\mathbf{E_m}^+$ and $k_{Am,+}$ would apparently require the L-serinamide zwitterion to be similarly reactive to hydroxide. Given that the L-serinamide zwitterion is, by our calculations, materially *less basic* than hydroxide, as well as considerably *more hindered*, a conventional assessment would seem to eliminate the zwitterion as the reactive species. Nevertheless, it should be noted that we cannot definitively discount the possibility – or see any trivial means of doing so – that intramolecular hydrogen bonding by a protonated α-amino group might profoundly enhance the reactivity of the β-hydroxyl group towards acylation by $\mathbf{E_m}$ (see SI for details). (b) Aziz, H. R; Singleton, D. A. Concert along the Edge: Dynamics and the Nature of the Border between General and Specific Acid–Base Catalysis. *J. Am. Chem. Soc*. **2017**, *139*, 16, 5965–5972.
(44) The effect of *N*-formylation on saponification ($k_{OH-,f}$/ $k_{OH-,0}$ = 11) is far more substantial than, but in the same direction as, that observed arising for the *N*-acetylation of L-phenylalanine methyl ester ($k_{OH-,f}$ / $k_{OH-,0}$ = 1.8; 25 °C, H_2O, I(NaCl) = 0.1M) [*Can. J. Chem*. **1971**, *49*, 3468-3476].
(45) Good, N. E.; Winget, G. D.; Winter, W.; Connolly, T. N.; Izawa, S.; Singh, R. M. M. Hydrogen Ion Buffers for Biological Research. *Biochemistry* **1966**, *5*, 467-477.
(46) No apparent racemisation of the stereogenic centre in the aminoacyl fragment was observed, by $^{19}F\{^1H\}_{IG}$ NMR, in the amide product obtained from L-serinamide and $\mathbf{E_m^f}$ at pH*(20°C) = 7.8. This suggests, but does not prove, that the oxazol-5(4H)-one of *N*-formyl-4-fluorophenylalanine is not a significant intermediate under our conditions (aminolysis); at the very least, the deprotonation of the oxazol-5(4H)-one, if actually formed from $\mathbf{E_m^f}$, must be considerably slower than its trapping by L-serianmide.
(47) Note that, empirically, hydrolysis is more significant in H_2O than D_2O, and thus amide yields are lower, primarily because of a large, normal equilibrium isotope effect on the autoprotolysis constant K_w. The inverse kinetic effects for saponification $(k_H/k_D)_{OL-}$ offset this normal effect, but only partially.
(48) (a) Wiberg, K. B. The Deuterium Isotope Effect. *Chem. Rev.* **1955**, *55*, 713-743. (b) Long, F. A. Acid Base Studies with Deuterium Oxide. *Ann. N. Y. Acad. Sci.* **1960**, *84*, 596-602. (c) Shiner Jr., V. J.; Mahler, H. R.; Baker Jr., R. H.; Hiatt, R. R. Secondary Deuterium Isotope Effects in Chemical and Biochemical Reactions. *Ann. N. Y. Acad. Sci.* **1960**, *84*, 583-595.

(d) Bunton, C. A.; Shiner, V. J., Jr. Isotope Effects in Deuterium Oxide Solution. Part II. Reaction Rates in Acid, Alkaline and Neutral Solution, Involving only Secondary Solvent Effects. *J. Am. Chem. Soc.* **1961**, *83*, 3207-3214.
(49) Bruice, T. C.; Fife, T. H. Hydroxyl Group Catalysis. III.1 The Nature of Neighboring Hydroxyl Group Assistance in the Alkaline Hydrolysis of the Ester Bond. *J. Am. Chem. Soc.* **1962**, *84* , 1973-1979.
(50) (a) Marlier, J. F. Heavy-atom isotope effects on the alkaline hydrolysis of methyl formate: the role of hydroxide ion in ester hydrolysis. *J. Am. Chem. Soc*. **1993**, *115*, 5953-5956. (b) Mata-Segreda, J. F. Hydroxide as General Base in the Saponification of Ethyl Acetate. *J. Am. Chem. Soc.* **2002**, *124*, 2259-2262.
(51) Barbara Schowen, K.; Schowen, R. L. Solvent isotope effects on enzyme systems. In *Methods in Enzymology*, Purich, D. L. Ed.; Vol. 87; Academic Press, 1982; pp 551-606.
(52) The fact that $\mathbf{E_m^f}$ and $\mathbf{E_m^0}$ share common solvent isotope effects for saponification and transesterification suggests that the corresponding transition states are quite analogous; that this is true is also suggested by their sharing almost identical activation parameters. The notably inferior intrinsic selectivity of $\mathbf{E_m^f}$ for transesterification appears, then, to be a consequence of steric hindrance. The correspondence of the activation parameters would also appear to discount any potential intramolecular general base catalysis of transesterification by the α-amino group in $\mathbf{E_m^0}$.
(53) Wang, B.; Zhou, J.; Lodder, M.; Anderson, R. D.; Hecht, S. M. Tandemly Activated tRNAs as Participants in Protein Synthesis. *J. Biol. Chem.* **2006**, *281*, 13865-13868.
(54) Neumann, H.; Shashoua, V. E.; Sheehan, J. C.; Rich, A. Intramolecular acyl migration in adenosine derivatives. *Proc. Natl. Acad. Sci. USA* **1968**, *61*, 1207-1214.
(55) These are again composite second-order rate constants: $k_{Am,Bis,++}$ is the sum of the individual constants for (formal) aminolysis at the 2'- and 3'-sites in $\mathbf{E_{Bis}}^{++}$, and $k_{Am,Bis,0}$ is the corresponding sum for $\mathbf{E_{Bis}^0}$. The constant $k_{Am,Bis,+}$ equals, to a good approximation, the *weighted* sum of the rate constants for the (formal) aminolysis of the 2'-aminoacyl ester in $\mathbf{E_{Bis,2'}}^{+}$ and the 3'-aminoacyl ester in $\mathbf{E_{Bis,3'}}^{+}$. See SI for full details.
(56) The pseudo first-order rate constants for aminolysis (k'_{Am}) and hydrolysis (k^{ψ}_{Hyd}) of the aminoacyl monoester, $\mathbf{E_m}$, obtained as a natural consequence of the kinetic deconvolution above, were in excellent agreement with the pH*-k'_{Am} and pH*-k^{ψ}_{Hyd} profiles obtained in separate studies initiated with $\mathbf{E_m}$ itself (see SI). Insufficient data were available to analyse pH*-k^{ψ}_{r} profiles.
(57) (a) Because we cannot distinguish *kinetically* between 2'- and 3'-protonation in $\mathbf{E_{Bis}}^{+}$, the *microscopic* pK_a* values for the 2'- and 3'-aminoacyl fragments determined by $^{19}F\{^1H\}$ chemical shift analysis must be weighted to give a single, "kinetic" pK_a* value each for $\mathbf{E_{Bis}}^{+}$ (pK_a*($\mathbf{E_{Bis}}^{+}$) and $\mathbf{E_{Bis}}^{++}$ (pK_a*($\mathbf{E_{Bis}}^{++}$). See SI for details of weighting, and the approximations used. (b) The value of pK_a*($\mathbf{E_m}^{+}$) (7.19; D_2O, 20°C, I = 2.0 M) determined by $^{19}F\{^1H\}$ chemical shift analysis and appropriate weighting (see SI) was in very good agreement with the value determined kinetically (Figure 4, Table 2; (pK_a*($\mathbf{E_m}^{+}$) = 7.08), and this correspondence gave us confidence to use similarly derived values for pK_a*($\mathbf{E_{Bis}}^{+}$) and pK_a*($\mathbf{E_{Bis}}^{++}$) as constrained parameters in fitting pH*-$k^{\psi}_{Hyd,Bis}$ and pH*-$k'_{Am,Bis}$.
(58) We encountered solubility issues with $\mathbf{E_{Bis}^f}$ that could be overcome with the co-addition of organic solvent (DMSO/acetonitrile) – but did not pursue detailed kinetic studies with this substrate due to the confounding effect associated with changing the medium.
(59) It is not clear what the pH of the solutions was in Hecht's study, though given that aqueous butylamine and imidazole were used (separately) as nucleophiles, it appears likely that pH > 10. This would fit with our observations.
(60) (a) Stepanov, V. G.; Moor, N. A.; Ankilova, V. N.; Lavrik, O. g. I. Phenylalanyl-tRNA synthetase from Thermus thermophilus can attach two molecules of phenylalanine to tRNAPhe. *FEBS Lett.* **1992**, *311*, 192-194. (b) Stepanov, V. G.; Moor, N. A.; Ankilova, V. N.; Vasil'eva, I. A.; Sukhanova, M. V.; Lavrik, O. g. I. A peculiarity of the reaction of tRNA aminoacylation catalyzed by phenylalanyl-tRNA synthetase from the extreme thermophile Thermus thermophilus. *Biochim. Biophys. Acta, Protein Struct. Mol. Enzymol.* **1998**, *1386*, 1-15.
(61) Janzen, E.; Blanco, C.; Peng, H.; Kenchel, J.; Chen, I. A. Promiscuous Ribozymes and Their Proposed Role in Prebiotic Evolution. *Chem. Rev.* **2020**, *120*, 4879-4897.
(62) Noller, H. F. The driving force for molecular evolution of translation. *RNA* **2004**, *10*, 1833-1837.

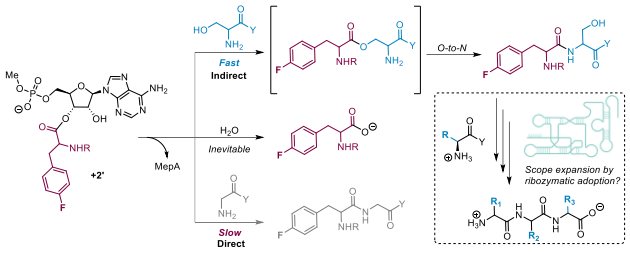
Me
NHR
+2'
MepA
Fast
Indirect
H2O
Inevitable
Slow
Direct
O-to-N
Scope expansion by
ribozymatic adoption?